CAD-RADS: Pushing the Limits

Arzu Canan, MD
Praveen Ranganath, MD
Harold Goerne, MD
Suhny Abbara, MD
Luis Landeras, MD
Prabhakar Rajiah, MBBS, MD, FRCR

Abbreviations: CAD = coronary artery disease, CAD-RADS = CAD Reporting and Data System, ECG = electrocardiography, ICA = invasive coronary angiography, LAD = left anterior descending, LCX = left circumflex, MPR = multiplanar reformatted, RCA = right coronary artery

RadioGraphics 2020; 40:629–652

https://doi.org/10.1148/rg.2020190164

Content Codes: CA CT SQ

From the Department of Radiology, Division of Cardiothoracic Imaging, UT Southwestern Medical Center, Dallas, Tex (A.C., P. Ranganath, H.G., S.A., P. Rajiah); Imaging and Diagnosis Center, Guadalajara, Mexico (H.G.); and Department of Radiology, University of Chicago Medical Center, Chicago, Ill (L.L.). Presented as an education exhibit at the 2018 RSNA Annual Meeting. Received May 22, 2019; revision requested June 27 and received August 16; accepted August 28. For this journal-based SA-CME activity, the authors, editor, and reviewers have disclosed no relevant relationships. **Address correspondence to** P. Rajiah, Department of Radiology, Mayo Clinic, 200 First St SW, Rochester, MN 55905 (e-mail: *radpr73@gmail.com*).

See discussion on this article by Aviram and Wolak (pp 653–655).

SA-CME LEARNING OBJECTIVES

After completing this journal-based SA-CME activity, participants will be able to:

- Discuss the different categories and modifiers of CAD-RADS classification.
- Describe clinical scenarios in which CAD-RADS guidance is not clear and understand the management of such scenarios.
- List the scenarios that are not currently addressed in the CAD-RADS.

See rsna.org/learning-center-rg.

Coronary CT angiography is now established as the first-line diagnostic imaging test to exclude coronary artery disease (CAD) in the population at low to intermediate risk. Wide variability exists in both the reporting of coronary CT angiography and the interpretation of these reports by referring physicians. The CAD Reporting and Data System (CAD-RADS) is sponsored by multiple societies and is a collaborative effort to provide standard classification of CAD, which is then integrated into patient clinical care. The main goals of the CAD-RADS are to decrease variability among readers; enhance communication between interpreting and referring clinicians, allowing collaborative determination of the best course of patient care; and generate consistent data for auditing, data mining, quality improvement, research, and education. There are several scenarios in which the CAD-RADS guidelines are ambiguous or do not provide definite recommendations for further management of CAD. The authors discuss the CAD-RADS categories and modifiers, highlight a variety of complex or ambiguous scenarios, and provide recommendations for managing these scenarios.

Online supplemental material is available for this article.

Introduction

Coronary CT angiography has grown exponentially since its introduction 2 decades ago, and multiple trials (1–7) have shown its clinical utility and improved outcomes. Coronary CT angiography is the first-line imaging examination for exclusion of coronary artery disease (CAD), with a high negative predictive value (8–11). It is used to characterize plaque and allows evaluation of other cardiac and extracardiac structures (12,13). Technologic advances continue to improve the capabilities of CT angiography. The latest scanners achieve spatial resolution of up to 0.25 mm and temporal resolution of up to 40 msec, with submillisievert radiation doses (14).

Obtaining high-quality images in an appropriately selected and prepared patient is only part of the job of a cardiac imaging practitioner. A high level of proficiency is also required to interpret the images accurately and provide guidance for decision making and management, without the need for follow-up examinations. Cardiac imaging practitioners communicate CT angiographic results to referring practitioners in written reports that can vary substantially, and this can inadvertently affect patient care. Ordering providers such as cardiologists address coronary CT angiographic findings appropriately, but general practitioners with less clinical expertise may find coronary CT angiographic results more challenging to interpret.

In 2016, multiple societies in the radiology and cardiology communities introduced the Coronary Artery Disease Reporting and Data System (CAD-RADS) as a collaborative effort. The initiative was sponsored by the Society of Cardiovascular Computed Tomography,

TEACHING POINTS

- The main goals of the CAD-RADS are to enhance communication between interpreting and referring clinicians, allowing collaborative determination of the best course of patient care, and to generate consistent data for auditing, data mining, quality improvement, research, and education.
- CAD-RADS categories 0, 1, and 2 represent nonobstructive CAD (ie, stenosis of less than 50% of the vessel), which does not require any further evaluation.
- A patient assigned to CAD-RADS category 4A requires either a functional test or ICA, whereas a patient with CAD-RADS 4B requires ICA..
- Four modifiers are used to complement the CAD-RADS categories and provide additional information.
- High risk (vulnerable) plaque features are positive remodeling, spotty calcification, napkin-ring sign, and low-attenuation plaque.

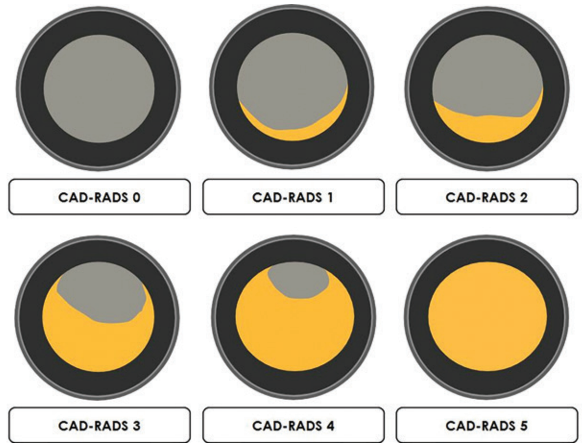

Figure 1. Illustration shows the five categories of CAD-RADS.

the American College of Cardiology, the American College of Radiology, and the North American Society for Cardiovascular Imaging (15). CAD-RADS is similar to other reporting systems that are used in radiology such as those for imaging the breasts (BI-RADS), liver (LI-RADS), lungs (Lung-RADS), and prostate (PI-RADS). CAD-RADS provides a standard classification of CAD, which is then integrated into patient-specific clinical care. The main goals of the CAD-RADS are to enhance communication between interpreting and referring clinicians, allowing collaborative determination of the best course of patient care, and to generate consistent data for auditing, data mining, quality improvement, research, and education. The CAD-RADS is not a substitute for the impression of the reporting physician, and findings should always be interpreted in combination with patient-specific information (15).

In this article, we begin by discussing the CAD-RADS categories and modifiers, with illustrative examples. In some situations in clinical practice, the correct CAD-RADS category is unclear. Furthermore, the CAD-RADS does not explicitly address several scenarios, including nonatherosclerotic causes of coronary artery narrowing, coronary artery anomalies, coronary dissection, and incidental findings. In the second part of this article, we address these situations and describe multiple clinical scenarios that illustrate the challenges encountered in application of the CAD-RADS guidelines.

CAD-RADS Categories

The CAD-RADS involves information derived from coronary CT angiography about the degree of stenosis, plaque characteristics, image quality, stents, and/or coronary artery bypass grafts. The CAD-RADS category is assigned on the basis of the most severe coronary finding in an individual patient at coronary CT angiography and ranges from 0 (absence of plaque) to 5 (at least one occlusion) (Fig 1). The category provides an interpretation of the findings and recommendations for further cardiac workup and management, which are different for stable and acute chest pain (Tables 1, 2).

CAD-RADS categories 0, 1, and 2 represent nonobstructive CAD (ie, stenosis of less than 50% of the vessel), which does not require any further evaluation (Figs 2–4). Alternative nonatherosclerotic causes of pain should be considered in patients with nonobstructive CAD. Stenosis that involves more than 50% of the vessel is classified as obstructive CAD and requires further evaluation. CAD-RADS 3 (Fig 5) represents moderate stenosis (50%–69%) of at least one coronary artery and requires further functional assessment to evaluate the hemodynamic effect of the stenosis. CAD-RADS 4A (Fig 6) is severe stenosis (70%–99%) of one or two coronary arteries, whereas CAD-RADS 4B (Fig 7) indicates significant (>50%) stenosis in the left main artery or severe stenosis (70%–99%) of three vessels. A patient assigned to CAD-RADS category 4A requires either a functional test or ICA, whereas a patient with CAD-RADS 4B requires ICA. Total occlusion of at least one of the vessels is classified as CAD-RADS 5 (Fig 8), and ICA and/or viability assessment is required. Category N refers to a nondiagnostic study (Fig 9), which means that at least one segment of the coronary arteries is not evaluable and the interpretable segments show less than 50% stenosis (CAD-RADS 0, 1, or 2). Only coronary vessels that measure more than 1.5 mm in diameter are evaluated with the CAD-RADS; smaller vessels are not evaluated (15).

Accurate CAD-RADS classification of coronary artery stenosis based on well-established guidelines is essential (16,17). Postprocessing

Table 1: CAD-RADS Classification for Patients with Stable Chest Pain

CAD-RADS Category	Interpretation	Degree of Maximal Coronary Stenosis	Further Cardiac Workup	Management
0	Absence of CAD	0%, no plaque or stenosis	None	Consider nonatherosclerotic causes of chest pain
1	Minimal CAD	1%–24%, minimal stenosis or plaque without stenosis	None	Consider nonatherosclerotic causes of chest pain Preventive therapy and risk modification
2	Mild CAD	25%–49%	None	Consider nonatherosclerotic causes of chest pain Preventive therapy and risk modification, especially for plaque in multiple segments
3	Moderate stenosis	50%–69%	Functional assessment	Consider symptoms-guided anti-ischemic and preventive pharmacotherapy and risk factor modification per guideline-directed care
4A	Severe stenosis	One or two vessels, 70%–99%	ICA or functional assessment	Consider symptoms-guided anti-ischemic and preventive pharmacotherapy and risk factor modification per guideline-directed care
4B	Severe stenosis	Left main artery >50% or three vessels ≥70%	ICA is recommended	Other treatments including revascularization should be considered per guideline-directed care
5	Total occlusion	100%	ICA and/or viability assessment	Same as for CAD-RADS 4A and 4B
N	Obstructive CAD cannot be excluded	Nondiagnostic	Additional or alternate evaluation	Additional or alternate evaluation

Source.—Reference 15.
Note.—Modifiers include N (nonevaluable segment), S (coronary stent), G (coronary bypass graft), and V (vulnerable plaque). ICA = invasive coronary angiography.

Table 2: CAD-RADS Classification for Patients with Acute Chest Pain

CAD-RADS Category	Likelihood of Acute Coronary Syndrome	Degree of Maximal Coronary Stenosis	Further Cardiac Workup	Management
0	Highly unlikely	0%	None	No further evaluation of acute coronary syndrome required; consider other causes
1	Highly unlikely	1%–24%	None	Consider evaluation of causes of non–acute coronary syndrome, if troponin level is normal and there are no ECG changes
2	Unlikely	25%–49%	None	Consider evaluation of causes of non–acute coronary syndrome, if troponin level is normal and there are no ECG changes
3	Possible	50%–69%	Functional assessment	Consider hospital admission with cardiology consultation, functional testing, and/or ICA
4A	Likely	One or two vessels 70%–99%	ICA or functional assessment	Consider hospital admission with cardiology consultation; further evaluation with ICA and revascularization, as appropriate
4B	Likely	Left main artery >50% or three vessels ≥70%	ICA is recommended	Consider hospital admission with cardiology consultation; further evaluation with ICA and revascularization, as appropriate
5	Very likely	100%	ICA and/or viability assessment	Consider expedited ICA and revascularization for acute occlusion
N	Cannot be excluded	Nondiagnostic	Additional or alternate evaluation	Additional or alternate evaluation for acute coronary syndrome

Source.—Reference 15.
Note.—Modifiers include N (nonevaluable segment), S (coronary stent), G (coronary bypass graft), and V (vulnerable plaque). ECG = electrocardiographic.

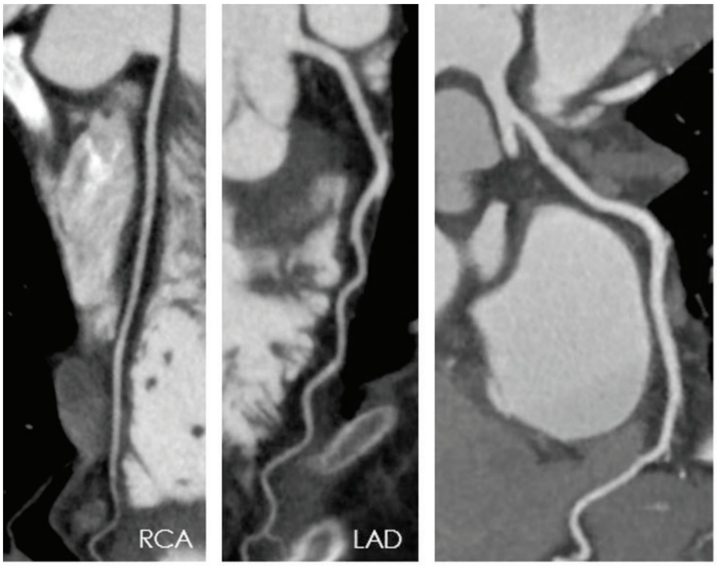

2a. **2b.** **2c.**

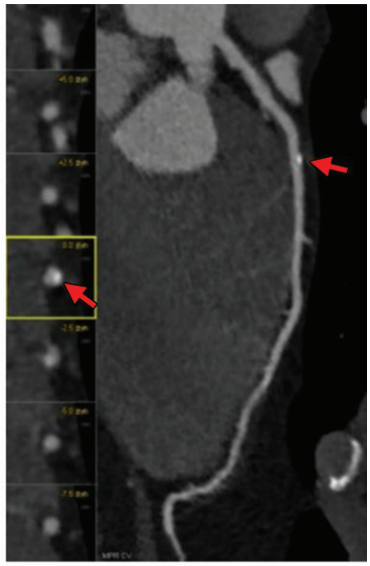

3.

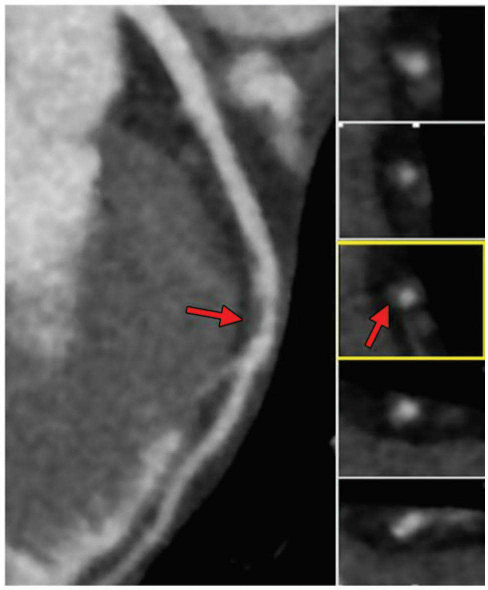

4.

Figures 2–4. **(2)** CAD-RADS 0 in a 59-year-old woman with a history of scleroderma and known cardiomyopathy. CT angiographic reconstructions of the right coronary artery (RCA) **(a)**, left anterior descending (LAD) artery **(b)**, and left circumflex (LCX) artery **(c)** reveal normal coronary arteries with no atherosclerotic disease or stenosis. No further imaging was recommended. **(3)** CAD-RADS 1 in a 41-year-old man with acute chest pain radiating to the left arm and dizziness. Curved multiplanar reformatted (MPR) CT angiographic image (right) and corresponding axial CT images (left) show a focal calcified plaque at the proximal LAD artery (arrows) that is causing minimal stenosis (<25%). No further imaging was recommended. **(4)** CAD-RADS 2 in a 60-year-old woman with recently diagnosed heart failure who was referred for the exclusion of CAD. Curved MPR CT image (left) and corresponding axial CT images (right) of the LAD artery reveal a noncalcified plaque (arrows) with mild stenosis (25%–49%). No further imaging was recommended.

software uses the axial CT images to generate oblique MPR images parallel and orthogonal to the stenotic coronary segments and curved MPR views along the centerline of the artery. The lesion is assigned a position on the basis of a standardized system of coronary artery segmentation (eg, the 18-segment model adapted by the Society of Cardiovascular Computed Tomography) (16,17). MPR views centered on the narrowest part of a stenosis (Fig 10) are used for subjective visual estimation of the percentage of luminal diameter of the stenosis relative to the nearest normal-appearing segment. Because coronary artery segments often have irregularly shaped lumina due to the eccentric positions of atherosclerotic lesions, the area rather than the diameter of stenosis may be more representative of the severity of luminal stenosis (18–20). However, stenosis diameter is preferred, because it is the standard for conventional coronary CT angiography. The minimal lumen diameter, minimal lumen area, and percentage of the area of stenosis can also be quantified (Fig 11). However, insufficient accuracy and reproducibility limit the use of these quantitative techniques in clinical practice (21,22). For this reason, CAD-RADS relies on qualitative rather than quantitative metrics of coronary stenosis.

An important challenge in accurate quantification of luminal stenosis is the presence of a densely calcified plaque, which typically results in overestimation of luminal stenosis due to calcium blooming artifacts caused by partial volume averaging (23). Calcium blooming artifacts can be reduced by means of several techniques that can be applied either before or after imaging (24). These techniques include increasing spatial resolution, average x-ray energy, or display window width. Spatial resolution can be improved by using a small collimator detector width, thin sections, a sharp reconstruction kernel (filter), or some model-based iterative reconstruction algorithms (Fig 12) (24,25). The

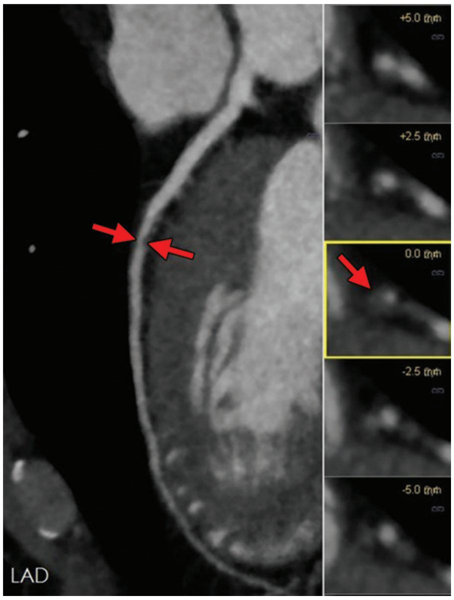

Figure 5. CAD-RADS 3 in a 65-year-old man with atypical chest pain. Curved MPR CT angiographic image (left) and corresponding axial CT images (right) show a noncalcified plaque (arrows) at the mid LAD artery that is causing moderate stenosis (50%–69%). Functional assessment was recommended. Myocardial perfusion scintigraphy (not shown) showed a stress perfusion defect in the apical anterior and inferior segments, which is consistent with ischemia.

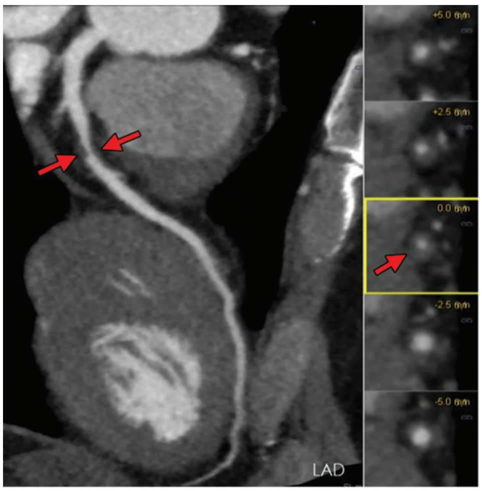

6.

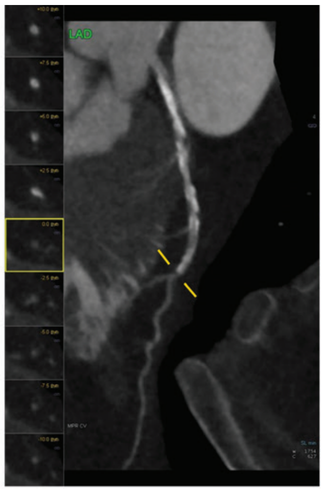

7a.

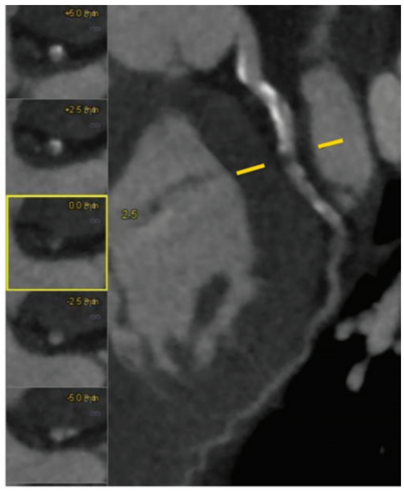

7b.

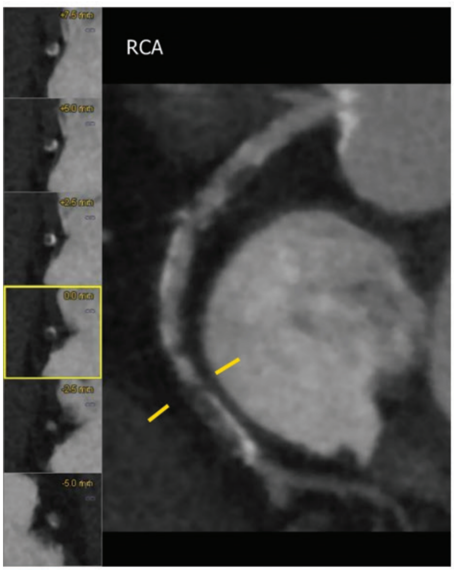

7c.

Figures 6, 7. **(6)** CAD-RADS 4A in a 48-year-old man who presented with chest pain on exertion and abnormal ECG results. Curved MPR CT angiographic image (left) and corresponding axial CT images (right) show a marked noncalcified plaque (arrows) in the mid LAD artery,with severe luminal stenosis (70%–99%). No other significant CAD was detected. ICA or functional assessment was recommended. ICA results (not shown) showed severe stenosis in the LAD artery, which was treated with balloon angioplasty and stent placement. **(7)** CAD-RADS 4B in a 60-year-old woman with diabetes mellitus and hyperlipidemia who presented with shortness of breath and chest pain. Curved MPR CT angiographic images (right) and corresponding axial CT images (left) of the LAD artery **(a)**, LCX artery **(b)**, and RCA **(c)** show severe stenosis (yellow markers). ICA results (not shown) confirmed three-vessel severe stenosis.

use of high x-ray energy (eg, 140 kVp) or high-energy virtual monoenergetic reconstructions acquired with a dual-energy CT scanner can also reduce calcium blooming artifacts (24,26). Algorithms are now available for accurate estimation of coronary artery stenosis in patients with heavily calcified coronary arteries (27).

The CAD-RADS also provides treatment recommendations that are specific to patients with stable and acute chest pain (Tables 1, 2).

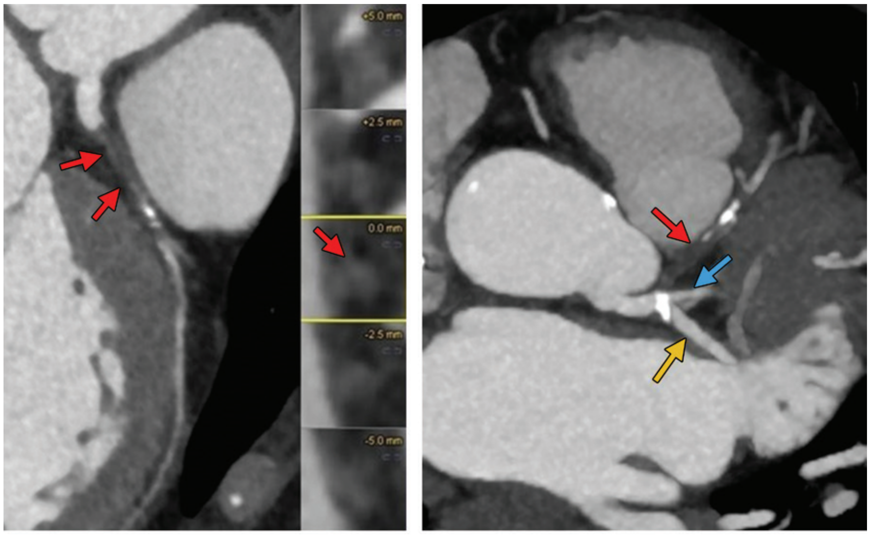

a. b.

Figure 8. CAD-RADS 5 in a 75-year-old woman who presented with acute chest pain but did not have ECG abnormalities. **(a)** Curved MPR CT angiographic image (left) and corresponding axial CT images (right) show diffuse atherosclerotic changes, with total occlusion of the proximal LAD artery (arrows). **(b)** Axial maximum intensity projection reconstruction (section thickness, 8 mm) of a CT angiographic examination also shows the occlusion of the proximal LAD artery (red arrow). Note the calcified plaque at the origin of the LCX artery (yellow arrow) and the large ramus intermedius (blue arrow). ICA findings (not shown) confirmed occlusion of the LAD artery. There was also minimal stenosis of the large ramus intermedius and moderate stenosis at the origin of the LCX artery.

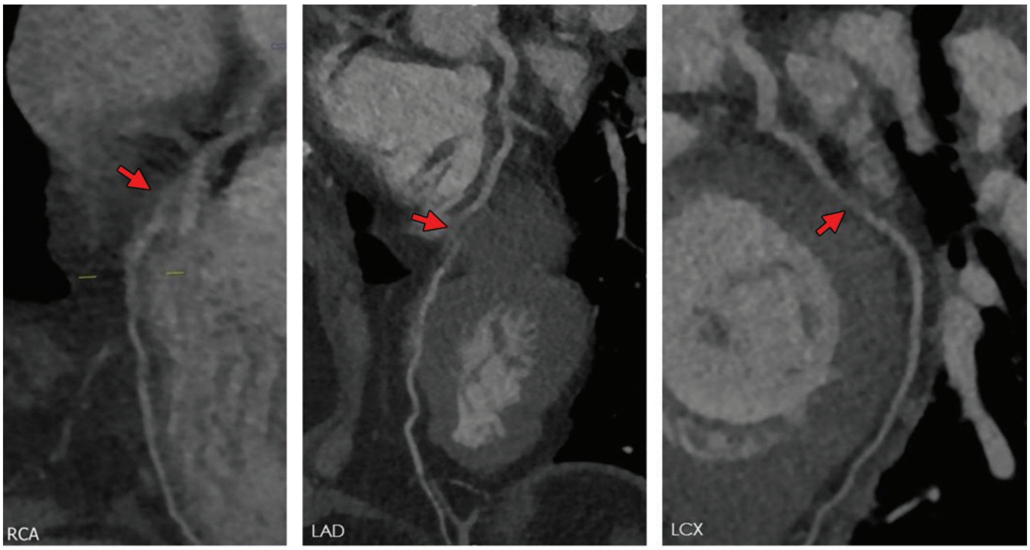

a. b. c.

Figure 9. CAD-RADS category N in a 62-year-old woman with a history of hypertension and hyperlipidemia who presented with chest pain on exertion and dyspnea. Coronary CT angiographic images show extensive motion artifacts (arrow) in the RCA **(a)**, LAD artery **(b)**, and LCX artery **(c)**. No atherosclerotic changes were noted in the diagnostic segments, but stenosis could not be excluded. Additional evaluation was recommended.

For patients with CAD-RADS categories 0, 1, and 2, alternate nonatherosclerotic causes of chest pain should be considered, and there is no need for additional imaging. In patients with stable chest pain, preventive therapy and risk factor modification are suggested for categories 1–5. Anti-ischemic therapy is recommended for CAD-RADS categories 3–5. Revascularization therapy is recommended for CAD-RADS categories 4 and 5.

In patients with acute chest pain, other causes of nonacute coronary syndrome should be considered for patients assigned CAD-RADS categories 0, 1, and 2. Hospital admission may be considered for patients with category 2, if there is high clinical suspicion of or high clinical risk for plaque features. Categories 3–5 require hospital admission and consultation with a cardiologist. Revascularization is appropriate for patients with CAD-RADS category 4 and should be expedited in those assigned to category 5 (15) (Tables 1, 2). Unlike therapy for stable chest pain, preventive therapy and risk factor modification are not recommended in the CAD-RADS guidelines for patients with acute chest pain. The SCOT-HEART (28) trial showed that the 5-year rate of death from

a.

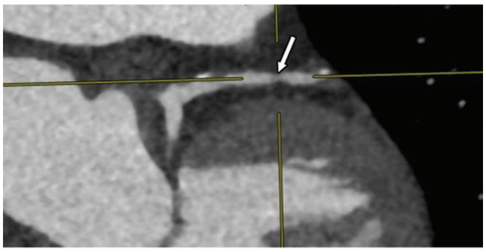

b.

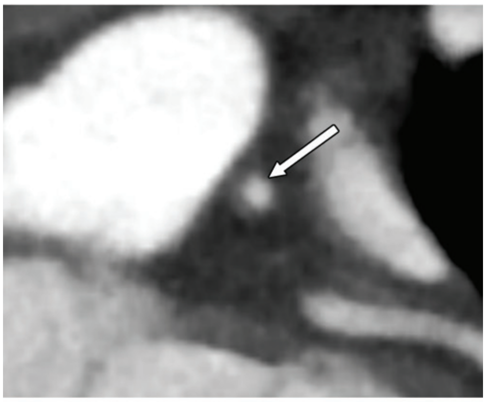

c.

Figure 10. Qualitative evaluation of coronary artery stenosis. **(a, b)** Curved MPR angiographic images of the LAD artery show stenosis (arrow) in the middle portion of the vessel **(a)**, and the most stenotic segment of the vessel **(b)** is centralized. **(c)** Corresponding axial reformatted CT image of that segment shows moderate stenosis (arrow).

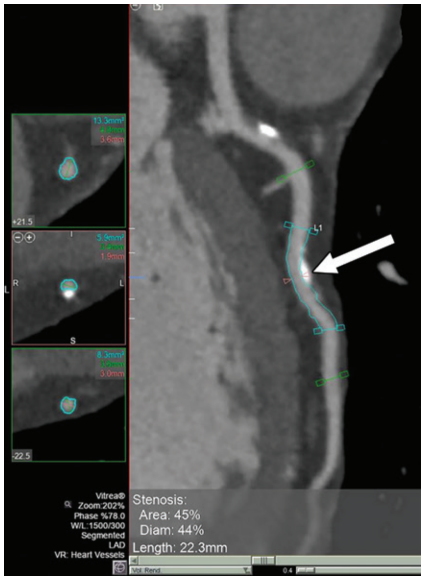

Figure 11. Quantitative evaluation of coronary artery stenosis. Curved MPR CT angiographic image (right) and corresponding axial CT images (left) show stenosis in the mid LAD artery (arrow). The stenotic lesion shows 44% obstruction, which is considered mild stenosis.

CAD or nonfatal myocardial infarction was significantly lower in patients who underwent coronary CT angiography for stable chest pain than in the standard care group. This finding emphasized the importance of preventive care in patients with stable chest pain, even in the absence of significant obstruction at coronary CT angiography.

Modifiers

Four modifiers are used to complement the CAD-RADS categories and provide additional information. These modifiers are nonevaluable (N), the presence of a stent (S) or a coronary bypass graft (G), and the presence of high-risk vulnerable plaque features (V). Multiple modifiers can be added to the category, separated by virgules (eg, CAD-RADS 3/N/S). When a nonevaluable segment is present in a coronary artery and there is significant stenosis (>50%) seen in another interpretable segment, the CAD-RADS score is dependent on the highest grade of stenosis in the study. In such a scenario, modifier N indicates the presence of the nonevaluable segment. The modifier S shows the presence of a coronary artery stent, regardless of the number and location of stents. Stents are present after 90% of percutaneous interventions (29) and can now be evaluated with CT angiography because of technologic advances (9,30,31). The evaluation of stenosis in a stent is similar to that in native coronary arteries. If the stent shows the highest grade of stenosis, then it is used to determine the CAD-RADS category. When the segment with the stent is nonevaluable, the modifier N is added.

The modifier G indicates the presence of a coronary bypass graft. Coronary CT angiography is an accurate modality for evaluating the patency of coronary bypass grafts (32–34). Stenosis at a bypass graft is graded similarly to grading of native coronary arteries. Conversely, stenosis that is bypassed by a fully patent graft is not considered for determination of the CAD-RADS category, because it does not have any effect on the myocardial blood supply (Fig 13).

a. b. c.

Figure 12. Calcium blooming artifact. Curved MPR maximum intensity projection CT angiographic images of the proximal LAD artery at a window width/window level of 1000/200 **(a)**, 1500/300 **(b)**, and 2700/900 **(c)** show a calcified plaque (arrow) with a decreased blooming artifact with the calcium-specific window width/window level and improved visualization of the vessel lumen.

High-risk atherosclerotic plaques are highly associated with acute coronary syndrome (35,36) (Fig 14). High-risk (vulnerable) plaque features are positive remodeling, spotty calcification, napkin-ring sign, and low-attenuation plaque. Positive remodeling is present when the vessel is enlarged at the site of the plaque compared with the proximal and distal vessel diameter. A plaque with attenuation of less than 30 HU is considered a low-attenuation plaque. Tiny punctate calcifications in the plaque are referred to as *spotty calcification*. The napkin-ring sign appears as a low-attenuation core surrounded by a rimlike area of high attenuation (37). This feature is more common in ruptured plaques and is specific in identification of a necrotic core (38). The modifier V is applied in the presence of at least two of these high-risk features in the same plaque (Fig 15). CAD-RADS does not provide specific guidelines for treatment of patients with high-risk coronary atherosclerotic plaques (15).

Challenging Situations in CAD-RADS

There are several clinical situations in which the choice of the correct CAD-RADS category or modifier is not clear. In the subsequent sections, we address these scenarios and make recommendations for appropriate management.

Scenario 1: Nonevaluable Segments at Coronary CT Angiography—Category N versus Modifier N

Case A.—A 71-year-old woman with stable angina underwent coronary CT angiography (Fig 16), which revealed no atherosclerotic disease at the left main, LAD, LCX, or proximal-mid right coronary arteries. The distal RCA could not be evaluated because of motion artifacts.

Case B.—A 78-year-old woman with chest pain underwent coronary CT angiography (Fig 17), which showed severe stenosis (70%–99%) at the mid LAD artery. The RCA could not be evaluated because of motion artifacts.

Comments.—The patient in case A was assigned CAD-RADS N, because there was no plaque in the interpretable segments of the coronary arteries and the mid RCA was nonevaluable. A significant plaque cannot be excluded in the nonevaluable segment. The presence of moderate to severe stenosis in this nonevaluable segment changes patient care. Alternative imaging was required to exclude CAD. In this scenario, if the study was performed with retrospective ECG gating, all of the available phases could have been evaluated, and techniques such as ECG editing could have been attempted before the study was labeled as nondiagnostic. On the other hand, if CT angiography was performed with prospective gating, the study may have been repeated with retrospective ECG gating and adequate premedication. There may be a phase with fewer or no motion artifacts (24). The patient in case B was assigned a CAD-RADS category of 4/N, because she already had severe stenosis, and further workup was needed to treat it. The nonevaluable segment did not change the need for invasive angiography. Hence, the modifier N is used instead of the category N.

The most common artifacts at coronary CT angiography are motion artifacts caused by cardiac, respiratory, or patient motion (24). A high heart rate and arrhythmia result in cardiac motion during the examination, which compromises image quality and leads to nonevaluable segments. Therefore, appropriate premedication before the examination to achieve a low and regular heart rhythm is essential to minimize motion artifacts and decrease the possibility of nonevaluable seg-

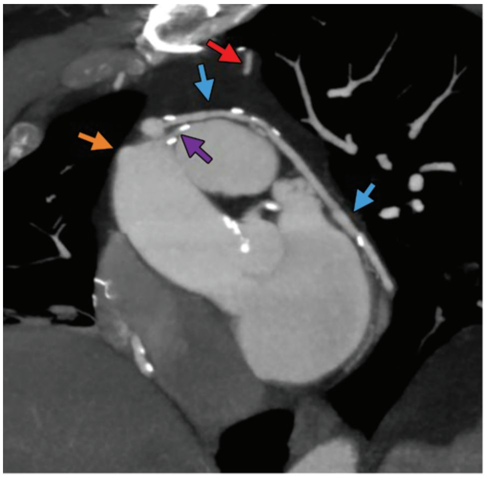

a.

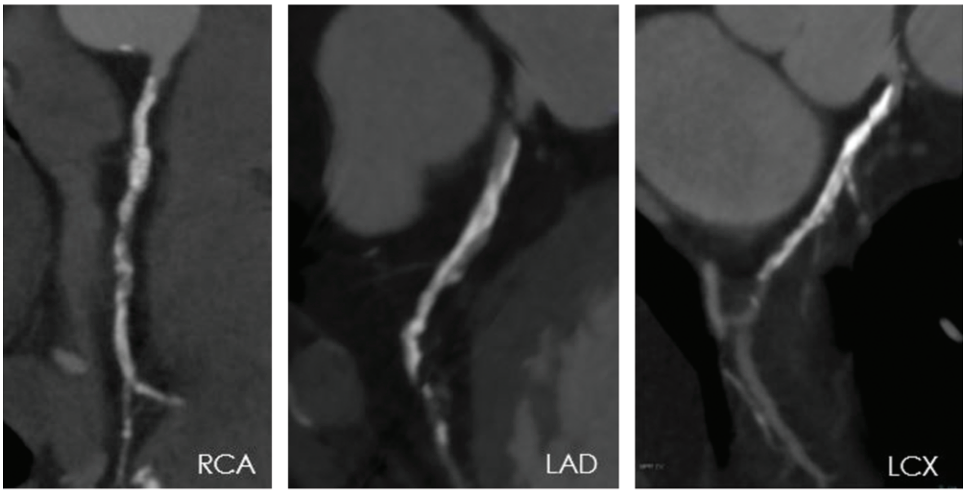

b. c. d.

Figure 13. Modifier G in a 77-year-old man with a history of four-vessel coronary bypass graft surgery who underwent coronary CT angiography to evaluate the patency of the grafts. **(a)** Sagittal oblique maximum intensity projection CT image shows saphenous venous grafts from the ascending aorta to the obtuse marginal artery (blue arrows) and to diagonal branches (purple arrow). Note the origin of the posterior descending artery graft (orange arrow) and the displacement of the left internal mammary artery (red arrow) from its original location, which is indicative of a graft from the left internal mammary artery to the LAD artery. All of the bypass grafts were patent. **(b–d)** Curved MPR CT images of the RCA **(b)**, LAD artery **(c)**, and LCX artery **(d)** show extensive calcification.

Figure 14. Illustration of vulnerable plaque features shows spotty calcification, the napkin-ring sign, low-attenuation plaque, and positive remodeling.

ments (24). Often, there are one or two distal segments with reduced image quality. Without any plaques in other vessels, these are potentially insignificant. However, following the CAD-RADS guidelines is recommended for any vessel with a diameter larger than 1.5 mm. No current evidence indicates that the outcomes of these lesions are less significant than those of proximal lesions.

Scenario 2: Significant Stenosis of the Left Main Coronary Artery

Case.—A 51-year-old woman with chest pain and elevated troponin levels underwent coronary CT angiography (Fig 18). No atherosclerotic plaques were found in the LAD artery, LCX artery, or RCA, but there was 60% stenosis in the left main artery.

Comments.—This patient was assigned CAD-RADS category 4B. Stenosis of greater than 50% in the left main coronary artery falls under category 4B, and ICA is needed for further evaluation. Revascularization should be considered.

Left main coronary artery stenosis, especially a significant obstructive lesion, is associated with higher mortality and morbidity rates than stenosis of other vessels because of the decreased blood supply of a larger myocardium (39,40). Similarly, the left main artery–specific calcium score was

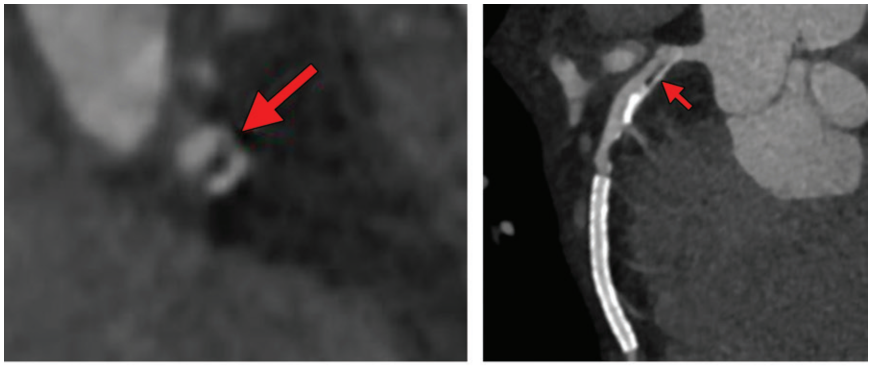

a. b.

Figure 15. Modifier V in a 64-year-old man with stable angina. Coronary CT angiography revealed a predominantly noncalcified plaque representing mild stenosis in the mid-LAD artery. **(a)** Axial MPR CT angiographic image shows the napkin-ring sign with high attenuation surrounding a lower-attenuation plaque (arrow). **(b)** Curved MPR CT angiographic image shows the napkin-ring sign and positive remodeling (arrow). A patent stent is also in place in the mid LAD artery. The patient was assigned CAD-RADS 2/S/V. No further imaging was recommended.

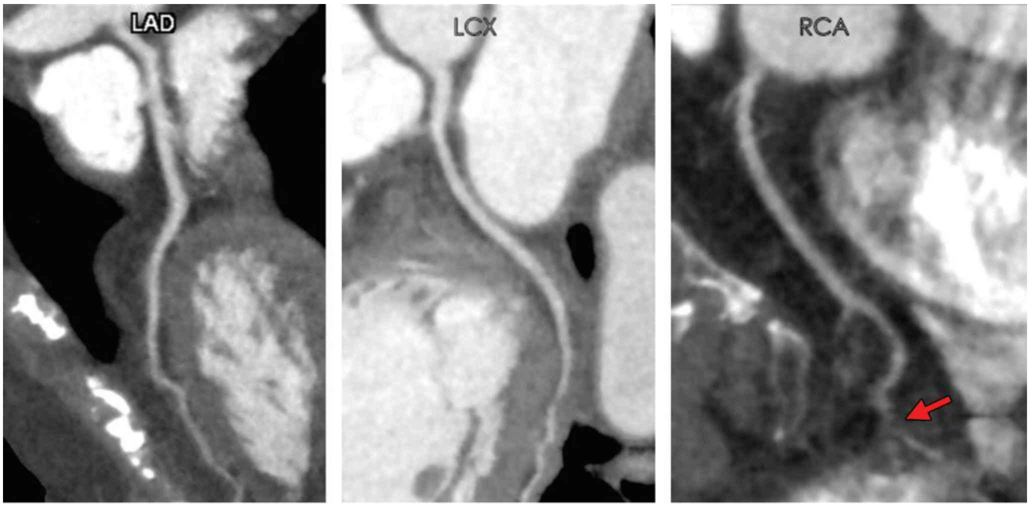

a. b. c.

Figure 16. CAD-RADS N in a 71-year-old woman. MPR CT angiographic images of coronary arteries show no atherosclerotic disease at the LAD artery **(a)**, the LCX artery **(b)**, or proximal to the mid RCA **(c)**. The distal RCA could not be evaluated because of a motion artifact (arrow in **c**). Additional or alternative evaluation was recommended.

found to be a significant predictor of all-causes mortality, with higher calcium scores associated with a higher risk of cardiovascular events (41). Therefore, revascularization of obstructive left main stenosis in symptomatic patients is the main treatment, either by means of coronary bypass graft surgery or percutaneous coronary intervention. Recent data (42) have shown no significant difference in the 5-year rate of mortality or major adverse cardiovascular events between coronary bypass graft surgery and percutaneous coronary intervention.

Scenario 3: Two-Vessel Disease at CT Angiography

Case.—A 63-year-old woman with dilated cardiomyopathy due to myotonic dystrophy had multiple calcified and noncalcified atherosclerotic plaques with severe stenosis in the proximal LAD artery and the LCX artery at coronary CT angiography (Fig 19). The RCA was a small vessel with minimal stenosis, and the posterior descending artery originated from the LCX artery (left dominant system). ICA results revealed severe stenosis of both the LAD and LCX arteries, and a nondominant RCA with minimal stenosis.

Comments.—The category assigned to this patient was CAD-RADS 4A. However, severe stenosis in the LAD and LCX arteries in a left-dominant system (ie, posterior descending artery originating from the left system) can cause a dramatic decrease in the myocardial blood supply. Hence, it is equivalent to three-vessel disease at ICA. Because the RCA anatomy can be evaluated at CT angiography, this scenario should be a three-vessel equivalent in CAD-RADS, which makes the correct category 4B and warrants the performance of ICA.

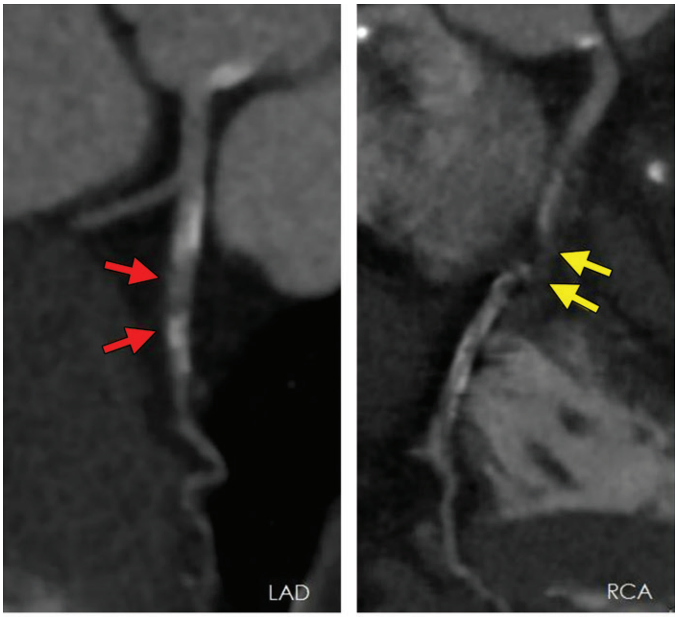

a. b.

Figure 17. CAD-RADS 4A/N in a 78-year-old woman with chest pain. **(a)** Coronary CT angiographic image shows severe stenosis (70%–99%) in the LAD artery only (arrows). **(b)** Coronary CT angiographic image shows that the RCA could not be evaluated because of motion artifacts (arrows). ICA or functional assessment was recommended. The patient underwent ICA (not shown), which confirmed severe stenosis (80%) at the LAD artery and also revealed moderate stenosis (50%–69%) in the mid RCA.

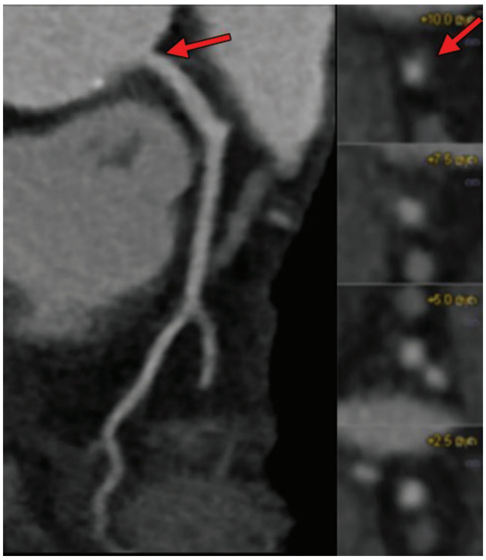

Figure 18. CAD-RADS 4B in a 51-year-old woman with chest pain and elevated troponin levels. Curved MPR (left) and corresponding short-axis (right) coronary CT angiographic images show moderate stenosis in the left main coronary artery (arrows). No other lesion was identified. ICA (not shown) results confirmed the moderate left main artery stenosis, without any other disease.

Scenario 4: High-Grade Stenosis in Small Vessels

Case.—Coronary CT angiography in a 68-year-old man with chest pain showed calcific plaques in the first diagonal branch of the LAD artery with possible severe stenosis. However, because of the small caliber of the vessel, the exact degree of stenosis could not be evaluated (Fig 20).

Comments.—CAD-RADS categories are applicable to coronary vessels that are larger than 1.5 mm. Vessels smaller than 1.5 mm are not represented by the CAD-RADS. Therefore, the possible severe stenosis in the first diagonal branch detected with CT angiography is not taken into consideration. Because there is no plaque or stenosis in the other coronary arteries, this patient was assigned a CAD-RADS category of 0, although there is demonstrable disease in the small coronary arteries.

Scenario 5: In-Stent Stenosis or Occlusion

Case.—A 70-year-old man with a history of inferior myocardial infarction and stent placement presented with new-onset chest pain (Fig 21). Coronary CT angiography showed a long-segment stent in the LCX artery, with total occlusion. The remaining segments of the LCX and other coronary arteries did not show obstructive disease.

Comments.—The CAD-RADS category is assigned on the basis of the highest grade of stenosis, which was total occlusion of a segment. Hence, this patient was assigned a CAD-RADS category of 5/S. ICA was recommended per guidelines, the results of which confirmed the total occlusion of the stent. In-stent stenosis or occlusion is evaluated similarly to evaluation of the native coronary arteries. In addition, the presence of a stent should be indicated by the modifier S. A CAD-RADS category 5 with a

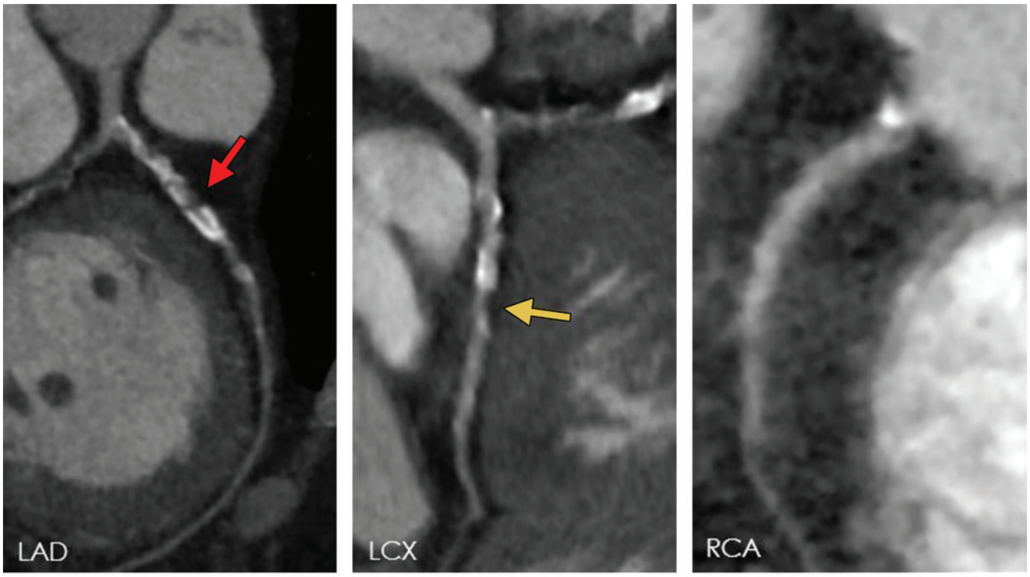

a. b. c.

Figure 19. Dilated cardiomyopathy in a 63-year-old woman. **(a, b)** Coronary CT angiographic images show a left-dominant system with the posterior descending artery originating from the LCX artery. Multiple calcified and noncalcified plaques are causing severe stenosis (70%–99%) of the proximal LAD (arrow in **a**) and LCX (arrow in **b**) arteries. **(c)** Calcified plaque with minimal stenosis was noted in the RCA. The patient was assigned CAD-RADS category 4A, and ICA or functional assessment was recommended. ICA results (not shown) confirmed severe stenosis of the LAD and LCX arteries and a nondominant RCA with minimal stenosis.

modifier S represents one of the following situations: *(a)* in-stent occlusion with patent native coronary arteries, *(b)* occlusion of a vessel and a patent stent in a different vessel, or *(c)* a patent coronary stent and a coronary occlusion in the nonstented portion of the same vessel. Because in-stent restenosis occurs in 20%–35% of patients with bare stents and 5%–10% of those with drug-eluting stents (43), evaluation of stent patency is a major concern for these patients. Although ICA is the standard method, noninvasive coronary CT angiography could provide similar information without the cost and complications of ICA. Despite the improved spatial and temporal resolution of the current CT applications, accurate assessment of stent patency is feasible only if the stent is larger than 3 mm in diameter (44). The classic appearance of in-stent restenosis is the lack of contrast (ie, hypoattenuation) in the stent lumen. Qualitative, semiquantitative, and quantitative methods have been described for evaluation of in-stent restenosis. The quantitative approaches depend on the comparison of the attenuation in the stent lumen with that of the vessel lumen before and after the stent is placed (45,46).

Scenario 6: Nonevaluable Stent

Case.—A 75-year-old man with stents in the LAD and first diagonal artery was evaluated with coronary CT angiography (Fig 22). The patency of the stent could not be evaluated because of extensive artifacts. A second stent at the diagonal branch was patent. The LCX artery and RCA also had small calcified plaques with minimal (<25%) stenosis.

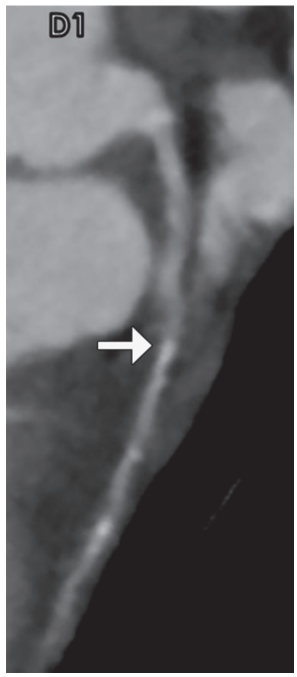

Figure 20. Stenosis in vessels smaller than 1.5 mm in diameter in a 68-year-old man with chest pain. Coronary CT angiographic image shows calcified plaque with luminal irregularity and possible severe stenosis in the first diagonal branch (arrow). Because of the small caliber of the vessel, correct interpretation of the stenosis was not possible. The other coronary arteries were normal. CAD-RADS categories are only assigned to vessels greater than 1.5 mm in diameter.

Comments.—This is an example of CAD-RADS N. Because of the artifacts, the evaluation of the stent was not possible, and there was no other significant stenosis detected at CT angiography.

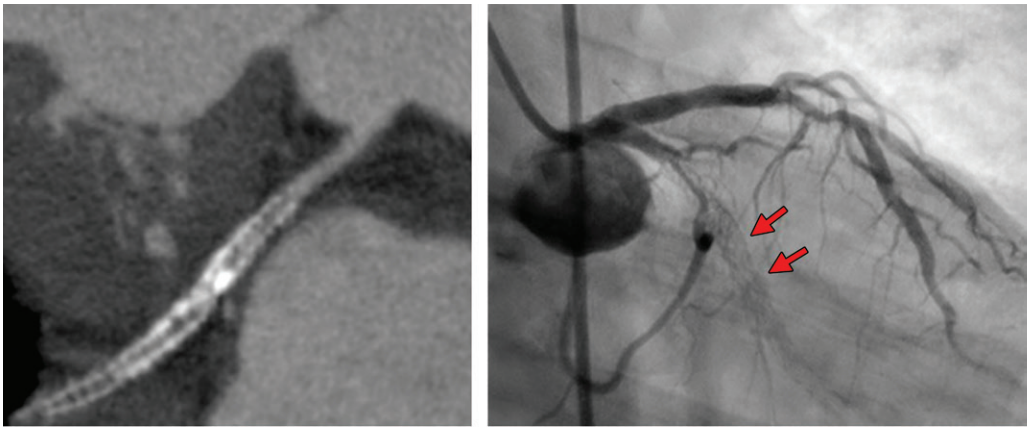

a. b.

Figure 21. CAD-RADS 5/S in a 70-year-old man with new-onset chest pain who had a history of inferior myocardial infarction and stent placement in the LCX artery. **(a)** Curved MPR CT angiographic image of the LCX artery shows a long stent in situ with a hypoattenuating lumen, which is consistent with total occlusion of the stent. **(b)** ICA image shows no flow in the stent (arrows), which confirms occlusion of the stent.

Thus, N should be used as a category instead of as a modifier. The uninterpretable part was a segment with a stent, but it did not change the choice of management.

Although 64-section CT has been shown to have 100% sensitivity and negative predictive value for the visualization of coronary stents, many factors affect stent visibility at coronary CT angiography, including the size of the stent, thickness of the struts, and presence of overlap (44,47). Larger stent diameter (>3 mm) and thinner stent struts have been shown to be significantly associated with more accurate evaluation of the stent lumen (31). In addition, stent struts could cause metallic artifacts that compromise image quality and assessment at CT angiography. The use of a high tube voltage or current, thinner sections, sharp kernel reconstructions, and iterative reconstructions might improve the image quality by eliminating metallic artifacts (48). In addition, the application of subtraction coronary CT angiography could provide higher diagnostic accuracy for evaluation of the stent (49).

Scenario 7: Severe Stenosis of a Graft

Case.—A 70-year-old man with known CAD and a history of coronary artery bypass graft surgery (Fig 23) underwent coronary CT angiography, at which a saphenous venous graft to the obtuse marginal branch and a left internal mammary artery graft to the LAD artery were detected. A calcified plaque that was causing severe stenosis was noted at the proximal portion of the saphenous graft. A patent stent at the distal portion of the same graft was present. The native coronary arteries were heavily calcified and occluded.

Comments.—Stenosis in a graft should be graded similarly to that in a native coronary artery, with modifiers S and G to describe the presence of the graft and stent. Also, stenosis in a native coronary artery that is bypassed by a fully patent graft is not considered for CAD-RADS classification, regardless of the degree of stenosis. Because this patient only had severe stenosis (70%–99%) in a single vessel, the category assigned was CAD-RADS 4A/S/G.

Coronary bypass graft surgery is the main treatment for advanced CAD. Saphenous veins, the internal mammary arteries, and the radial arteries are the main vessels that are used for coronary bypass grafts. Saphenous vein grafts are more prone to atherosclerosis than are internal mammary artery and radial artery grafts, which have higher rates of long-term patency (50).

Other than the graft type, the plaque burden in the native coronary arteries has been found to increase the risk of graft stenosis. Graft stenosis occurs more frequently in patients with diffuse native coronary artery atherosclerosis than in those with focal atherosclerotic disease (51). Coronary CT angiography is the main noninvasive imaging method to evaluate graft patency, with high diagnostic accuracy (52,53).

Scenario 8: Graft with Occlusion, Stenosis, or Stent

Case.—A 60-year-old man with known three-vessel disease and a history of coronary artery bypass graft surgery with saphenous venous grafts to the LAD artery and the obtuse marginal branches underwent coronary CT angiography (Fig 24). A stent was detected in the saphenous venous graft to the obtuse marginal branch of the LCX artery. The saphenous venous graft to the LAD artery

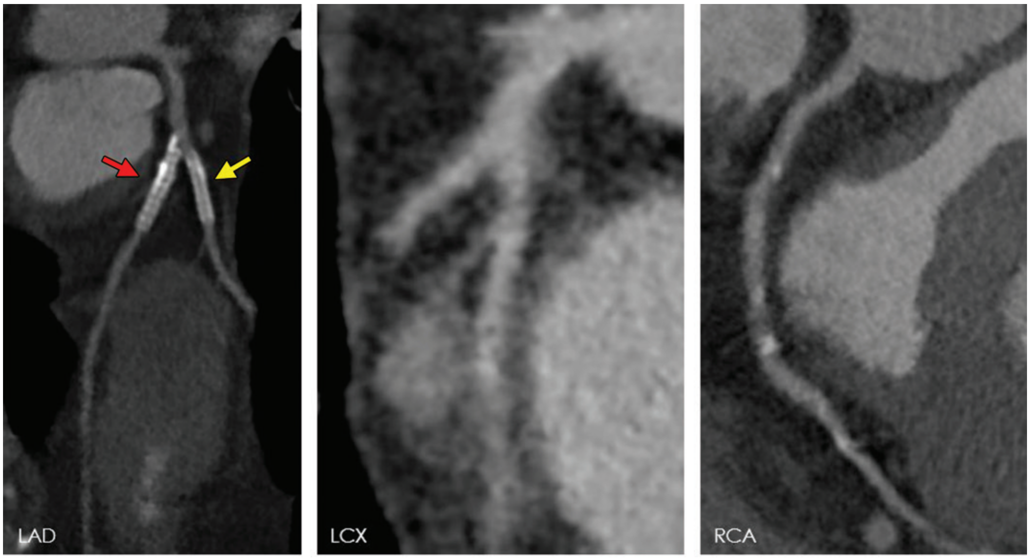

a. b. c.

Figure 22. CAD-RADS N/S in a 75-year-old man with a history of myocardial infarction and stent placement who presented with chest pain. **(a)** Coronary CT angiographic image shows minimal calcification at the stent in the mid LAD artery (red arrow). Luminal evaluation for the presence and severity of stenosis could not be performed because of poor contrast material opacification (yellow arrow). **(b, c)** Coronary CT angiographic images show small calcific plaques with minimal stenosis in the LCX artery **(b)** and the RCA **(c)**. Additional or alternate evaluation was recommended.

was totally occluded at its ostium. The native coronary arteries were heavily calcified and occluded.

Comments.—Graft stenosis or occlusion or the presence of a stent in a graft is not specified in the CAD-RADS classification. Total occlusion of any vessels, including grafts or stents, results in classification as CAD-RADS 5. The presence of a graft and a stent means that S and G are added, and thus the patient was assigned CAD-RADS 5/S/G. The total occlusion could be in *(a)* a nongrafted segment of the native coronary artery, *(b)* a stent in a native coronary artery or a stent in a graft, or *(c)* a coronary artery bypass graft. Because of its high spatial and temporal resolution, coronary CT angiography is the most established and effective noninvasive method to evaluate coronary artery stents, coronary bypass grafts, and native coronary arteries (54).

Scenario 9: Two High-Risk Features in Different Plaques

Case.—A 42-year-old man with chronic chest pain had a significant family history for CAD. He underwent coronary CT angiography, which showed noncalcified plaque with positive remodeling in the LAD artery (Fig 25a) that caused mild stenosis and multiple small calcified plaques and spotty calcifications, with minimal stenosis in the RCA (Fig 25b).

Comments.—This patient was assigned a CAD-RADS category of 2, with no modifier. Although there were two high-risk plaque features, they were seen in different plaques. Modifier V is assigned only if there are two high-risk features in the same atherosclerotic plaque. Therefore, this patient was assigned CAD-RADS 2 without a modifier, which represents only mild stenosis of the mid LAD artery. Because high-risk plaque features have been shown to be early predictors of future cardiovascular events, especially acute coronary syndrome, describing and reporting these features is important (56,57). Although the definition of modifier V requires the presence of at least two of those high-risk features, studies have show that the napkin-ring sign alone is the most significant predictor of acute coronary syndrome, independent of other high-risk features (58). In addition, low-attenuation plaque, especially less than 60 HU, is the second most powerful predictor, after the napkin-ring sign, of future events (56).

Limitations of CAD-RADS Classification

Scenario 10: Stent Complications

Case.—A 47-year-old woman with a history of myocardial infarction and stent placement presented with acute chest pain. Coronary CT angiography showed evidence of fracture of the coronary stent (Fig 26) and mild narrowing at the origin of the first diagonal branch of the LAD artery.

RadioGraphics

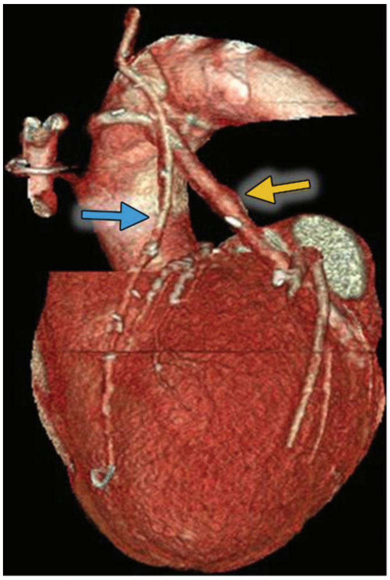

a.

Figure 23. CAD-RADS category 4A/S/G in a 70-year-old man with a known myocardial infarction who underwent coronary bypass graft surgery and presented with chest pain. **(a)** Three-dimensional volume-rendered CT image shows the saphenous vein graft (SVG) from the ascending aorta to the obtuse marginal (OM) branch (yellow arrow) and the arterial graft from the left internal mammary artery (LIMA) to the LAD artery (blue arrow). **(b)** Curved MPR CT angiographic image shows the distal patent stent (red arrow) and proximal severe stenosis (white arrow) in the SVG from the aorta to the OM branch (yellow arrows). **(c)** Curved MPR CT angiographic image shows that the graft from the LIMA to the LAD artery (arrows) is patent, with multiple surgical clips along the length of the graft. ICA or functional assessment was recommended.

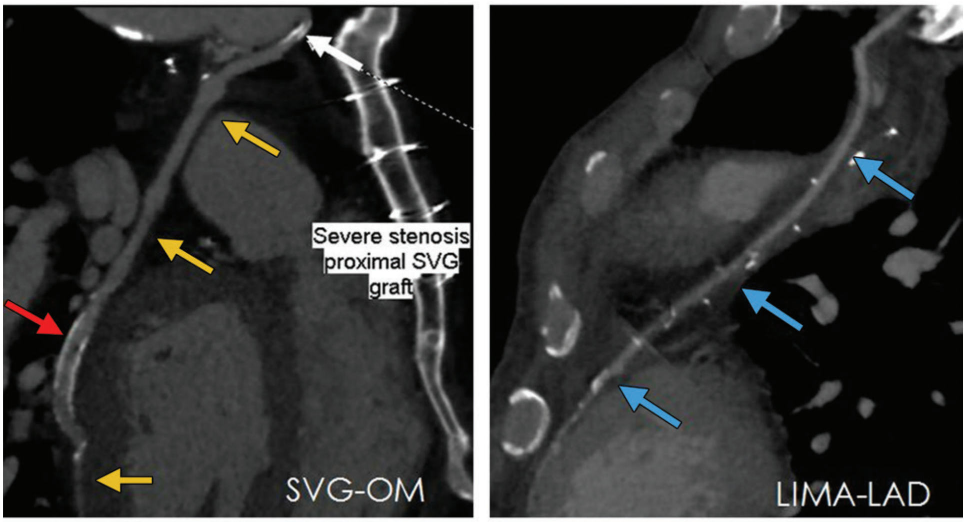

b. c.

Comments.—The category assigned to this patient was CAD-RADS 2/S, which represents mild narrowing of the first diagonal branch and the presence of a coronary stent. However, a limitation of CAD-RADS is that it does not provide information about stent or graft complications. A stent fracture is defined as a partial or complete gap in the stent with attenuation of less than 300 HU at CT angiography. Stent fractures are detected more frequently at coronary CT angiography than at ICA (58). Although advances in stent technology have decreased the incidence of fractures, they still occur in 0.8%–8% of stents (59). Coronary CT angiography accurately shows stent complications, including stent fracture and overlapping. CAD-RADS classification includes the presence of a stent and evaluation of in-stent restenosis but does not address other complications of stents, such as fractures (60,61).

Scenario 11: Volume of Plaque and Multiple Plaques

Case A.—A 73-year-old man with chest pain underwent coronary CT angiography, which revealed a single calcified plaque with moderate stenosis in the proximal LAD artery (Fig 27a).

Case B.—Coronary CT angiography in a 66-year-old man with known coronary artery calcification and abnormal tolerance test results showed multiple calcified and noncalcified long-segment plaques in all of the coronary arteries, with moderate stenosis in the mid LAD artery (Fig 27b–27d).

Comments.—Although both of these patients had moderate stenosis and were assigned CAD-RADS 3, patient B had a higher plaque volume

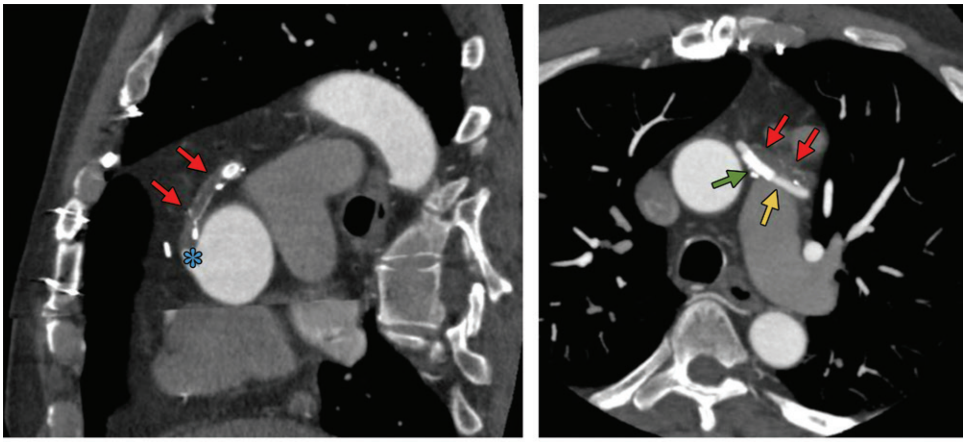

a. b.

Figure 24. CAD-RADS 5/S/G in a 60-year-old man with known severe three-vessel disease, after he underwent coronary artery bypass graft surgery. Sagittal oblique MPR **(a)** and axial maximum intensity projection **(b)** coronary CT angiographic images show saphenous venous grafts from the ascending aorta to the LAD artery (red arrows) and from the ascending aorta to the obtuse marginal branch of the LCX artery (yellow arrow in **b**). The saphenous venous graft to the LAD artery is totally occluded beyond its ostium (* in **a**). A patent stent (green arrow in **b**) is detected at the saphenous venous graft to the OM branch. ICA was recommended.

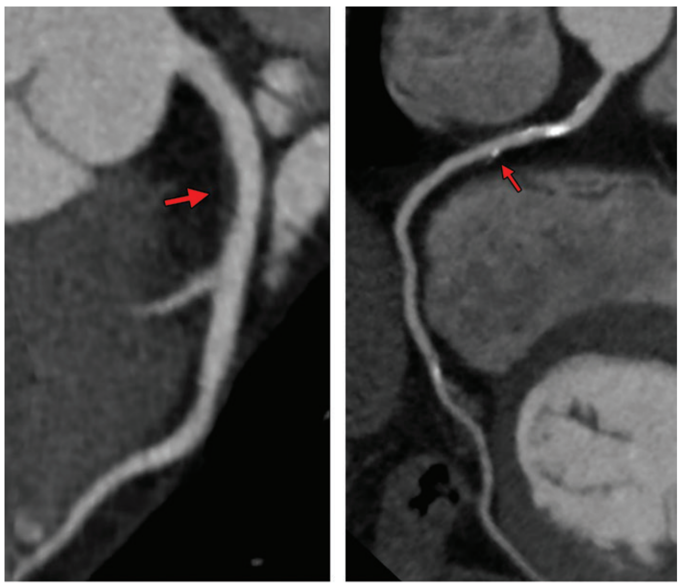

a. b.

Figure 25. CAD-RADS 2 in a 42-year-old man with chest pain and a significant family history of CAD. **(a)** Coronary CT angiographic image shows a noncalcified plaque in the proximal LAD artery, with positive remodeling (arrow) and mild stenosis. **(b)** Coronary CT angiographic image also shows multiple small plaques with minimal stenosis and spotty calcification (arrow) in the RCA. There are two high-risk features, but they are seen in different plaques, so the CAD-RADS score does not include the modifier V. No further imaging was recommended.

than did patient A. The CAD-RADS does not have a category or modifier for the volume of atherosclerotic plaque, and only the highest grade of stenosis is considered. However, the total plaque volume has also been found to be a predictor of acute coronary syndrome (62). Higher total plaque volume and the presence of noncalcified plaque have been suggested as findings that allow discrimination of acute coronary syndrome from stable CAD (63). Furthermore, higher noncalcified plaque burden was found to be associated with increased perfusion defects (64). Hence, plaque characterization and estimation of total plaque volume are essential components of interpretation of coronary CT angiography.

Scenario 12: Coronary Artery Anomalies

Case A.—A 66-year-old man who was undergoing hemodialysis for end-stage renal disease before kidney transplant underwent coronary CT angiography, which revealed a few calcified plaques in the proximal and mid LAD artery that were causing mild stenosis. The RCA abnormally originated from the anteromedial ascending aorta (an abnormally high origin) and the proximal part had an interarterial course between the

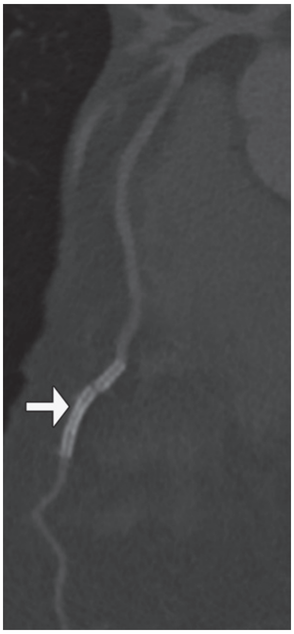

Figure 26. CAD-RADS 2/S in a 47-year-old woman. Curved MPR CT angiographic image of the LAD artery shows a coronary artery stent (arrow) at the distal portion of the vessel, with a complete gap in and angulation of the stent due to fracture.

ascending aorta and the main pulmonary artery (interarterial course) (Fig 28a).

Case B.—A 32-year-old man with chest pain and a history of familial hypercholesterolemia underwent CT angiography, which showed no atherosclerotic changes but did show deep myocardial bridging at the mid LAD artery, coursing through the interventricular septum and extending into the right ventricular cavity (Fig 28b).

Comments.—Case A is an example of CAD-RADS category 2 due to the presence of mild stenosis of the LAD artery. Case B was assigned a CAD-RADS category of 0, because the patient did not have any atherosclerotic plaque or stenosis. Both of those patients had nonstenotic coronary artery findings, but CAD-RADS classification does not take into account those findings.

Congenital coronary anomalies are detected at coronary CT angiography, with a prevalence of approximately 1%–1.7% (65–67). The clinical manifestation of coronary artery anomalies varies from an incidental finding to sudden cardiac death (68). Coronary CT angiography has been shown to be an accurate and noninvasive method to detect coronary anomalies and to show their origin, course, and termination. It also establishes their relationship with the surrounding structures (69). Coronary artery anomalies such as the interarterial course, intramural course, and acute angulation are associated with a higher risk of myocardial infarction, but there are no CAD-RADS categories for these anomalies. Hence, they should be reported separately and mentioned in the impression (70).

Scenario 13: Nonatherosclerotic Causes of CAD

Case.—A 34-year-old woman with sudden-onset chest pain underwent coronary CT angiography, which showed linear hypoattenuation in the lumen, indicating spontaneous dissection of the LAD artery and no atherosclerotic disease (Fig 29).

Comments.—Although this patient had coronary artery dissection, which accounted for her chest pain, she was assigned a CAD-RADS category of 0 because of the absence of atherosclerotic plaque and stenosis. Atherosclerosis is the leading cause of coronary artery stenosis. However, a small percentage of patients with myocardial ischemia do not show atherosclerotic plaques at coronary CT angiography or ICA. Of all myocardial infarctions, 4%–7% occur because of congenital or acquired nonatherosclerotic disease that results in severe coronary artery narrowing. The percentage is four times higher in patients who are younger than 35 years (71). There are three broad mechanisms by which the coronary arteries can be compromised by nonatherosclerotic disease (Table 3) (Fig 30). Extrinsic compression of the coronary artery and reduced coronary artery blood flow can be caused by a myocardial bridge, an adjacent mass, or severe dilatation of the pulmonary artery (72,73). Intrinsic luminal narrowing and limited coronary blood supply can be caused by vasculitis, fibromuscular hyperplasia, or coronary artery dissection (72). A flow reduction due to mismatch between myocardial oxygen demand and supply can be caused by coronary artery anomalies such as an anomalous coronary artery origin from the pulmonary artery (70,74).

Coronary CT angiography is the modality of choice for evaluation of nonatherosclerotic causes of coronary artery narrowing owing to the ability to assess the vessel wall and surrounding structures in addition to vessel lumen. Moreover, it can reveal the mechanism of blood flow reduction. Although all of these findings of nonatherosclerotic narrowing are readily shown at CT angiography, the CAD-RADS does not mention the exact mechanism or cause of coronary artery stenosis.

Scenario 14: Coronary Artery Ectasia and Aneurysm

Case A.—A 58-year-old woman with stable chest pain underwent coronary CT angiography, which revealed ectasia of the right coronary artery (Fig 31). No stenosis or plaque of the coronary arteries was noted.

Case B.—An 83-year-old man with cardiomyopathy, fatigue, and shortness of breath underwent

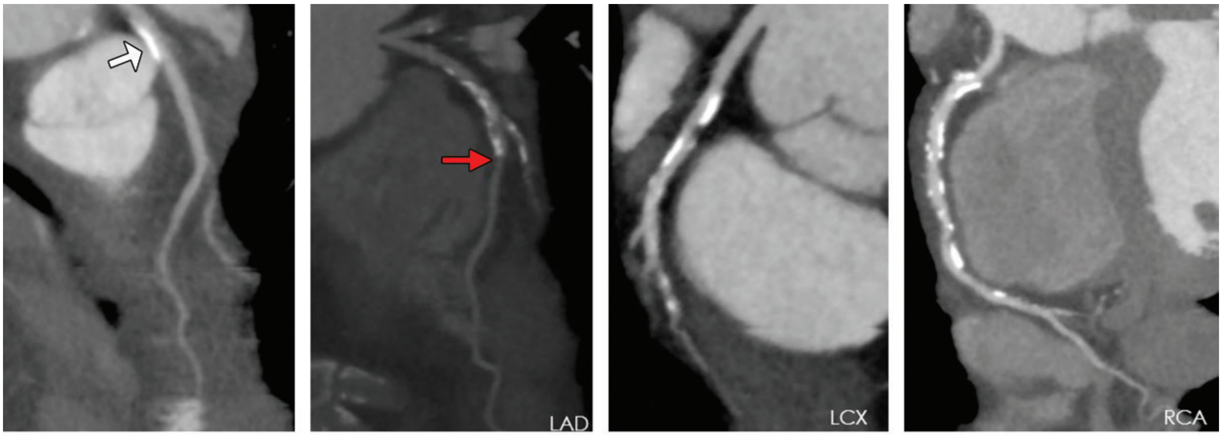

a. b. c. d.

Figure 27. CAD-RADS 3 in two patients. **(a)** Curved MPR coronary CT angiographic image in a 73-year-old man with chest pain shows a calcific plaque in the proximal LAD artery (arrow), with associated moderate luminal stenosis. **(b–d)** Curved MPR coronary CT angiographic images of the LAD artery **(b)**, the LCX artery **(c)**, and the RCA **(d)** in a 66-year-old man show diffuse atherosclerotic disease in all of the coronary arteries, with moderate stenosis in the mid LAD artery (arrow in **b**). Although the plaque burden in the two patients differed, they were both assigned CAD-RADS 3, and functional assessment was recommended for both.

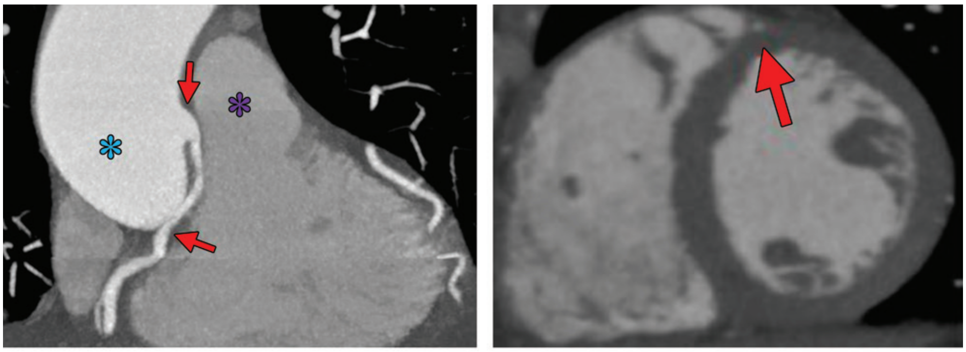

a. b.

Figure 28. Coronary artery anomalies in two patients. **(a)** Coronal oblique maximum intensity projection coronary CT angiographic image in a 66-year-old man shows an anomalous origin of the RCA (arrows) high above the sinotubular junction. The proximal RCA has an interarterial course from the ascending aorta (blue *) and pulmonary trunk (purple *). **(b)** Short-axis CT image of the left ventricle in a 32-year-old man shows deep myocardial bridging of the mid LAD artery (arrow), which extends into the left ventricular myocardium. CAD-RADS does not apply to these findings, so the patient was assigned a CAD-RADS category of 0.

coronary CT angiography, which showed diffuse scattered calcifications with mild stenosis in the LAD artery and a focal aneurysm in the proximal LAD artery (Fig 32). Additional mild stenosis in the RCA and LCX artery were noted.

Comments.—The category of patient A was CAD-RADS 0 and that of patient B was CAD-RADS 2. Coronary artery ectasia and aneurysm are not accounted for in CAD-RADS classification. There are no specific recommendations for further imaging or management of coronary artery ectasia or aneurysm.

Coronary artery ectasia or aneurysm occur when there is an enlargement of the coronary artery with a diameter of 1.5 times more than the normal diameter of the artery. Ectasia involves more than 50% of the vessel length, whereas coronary artery aneurysm is only focal dilatation that includes less than 50% of the vessel length (75). Atherosclerosis is the most common cause of both coronary artery ectasia and aneurysms, followed by congenital infectious diseases in Western countries, whereas Kawasaki disease is the leading cause in Asia (76). The clinical importance of ectasia or aneurysm caused by atherosclerosis depends on the degree of associated coronary artery stenosis. The investigators in the Coronary Artery Surgery Study registry have found no difference in 5-year survival in patients with and without aneurysms who had occlusive CAD (77). Thus, CAD-RADS classification and management recommendations only take into account the highest degree of associated coronary artery stenosis but not the presence of ectasia or aneurysm.

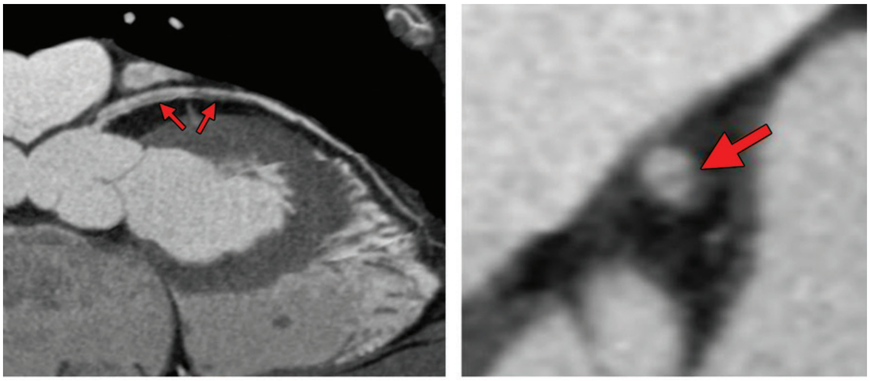

a. b.

Figure 29. CAD-RADS 0 in a 34-year-old woman with acute chest pain. Curved MPR **(a)** and corresponding axial **(b)** CT angiographic images show a linear hypoattenuating lesion (arrows) in the LAD artery lumen that indicates coronary artery dissection with associated moderate luminal stenosis. The patient was assigned CAD RADS 0, because she did not have any atherosclerosis. ICA results (not shown) confirmed spontaneous coronary artery dissection of the LAD artery.

Table 3: Nonatherosclerotic Causes of Coronary Artery Narrowing

Type of Coronary Artery Narrowing
Extrinsic compression
Interarterial course
Myocardial bridge
Mass (neoplastic or nonneoplastic)
Loop (kink)
Severe dilatation of pulmonary artery
Intrinsic compression
Embolus
Coronary dissection
Vasculitis
Fibromuscular hyperplasia
Idiopathic calcification
Flow reduction
High origin
Ostial obstruction
Vasospasm
Anomalous left coronary artery originating from pulmonary artery, and/or anomalous right coronary artery originating from pulmonary artery
Myocardial infarction with nonobstructive coronary arteries
Fistula

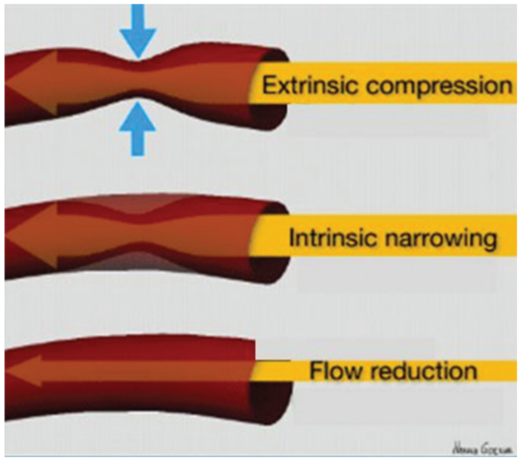

Figure 30. Illustration shows the nonatherosclerotic mechanisms of coronary artery stenosis, which may be caused by extrinsic compression, intrinsic narrowing, or flow reduction.

Scenario 15: Hemodynamic Significance of the Stenosis

Case A.—A 53-year-old man with chest pain underwent cardiac CT perfusion imaging at rest and under stress after infusion of adenosine. A perfusion defect was seen in the anterolateral wall in the stress images but not in the rest images, which is indicative of myocardial ischemia (Fig 33a).

Case B.—Coronary CT angiography in a 66-year-old man with stable angina showed moderate LAD artery stenosis. CT fractional flow reserve analysis of the same lesion revealed a value of 0.67, which indicated hemodynamically significant stenosis (Fig 33b).

Comments.—CAD-RADS does not include the hemodynamic assessment of stenosis, which is now possible with CT. These patients are assigned CAD-RADS categories on the basis of the highest grade of stenosis. Significant stenosis at coronary CT angiography does not necessarily mean that it is the culprit lesion that led to myocardial ischemia, because there is a mismatch between CT angiographic findings and ischemia. Severe stenosis at CT angiography may be predictive of future events such as myocardial infarction or death. The location, severity, and nature of stenosis; the cumulative degree of obstructive disease; microvascular status; and the health and viability of the myocardial bed and ischemia are other factors to be considered (78). Detection of hemodynamically significant stenosis is important to guide patient treatment with revascularization of the lesion, which relieves symptoms and prevents further myocardial damage. Functional

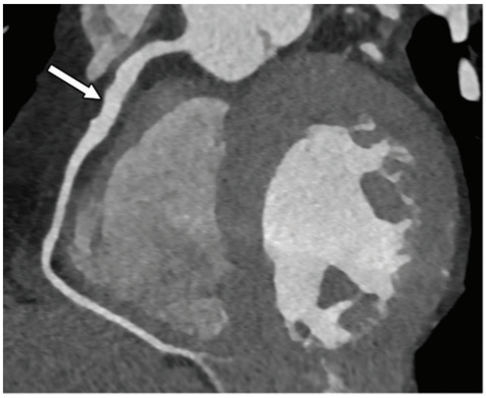

31.

32.

Figures 31, 32. **(31)** Curved MPR angiographic image of the RCA in a 58-year-old woman with chest pain shows ectasia of the right coronary artery (arrow) without any coronary artery plaques or stenosis. The patient was assigned CAD-RADS 0. No further imaging was recommended. **(32)** Curved MPR angiographic image of the LAD artery in an 83-year-old man with cardiomyopathy, fatigue, and shortness of breath shows diffuse scattered calcified plaques with a focal aneurysm of the LAD artery (arrow), which measured 8 mm in diameter. Mild stenosis of the RCA and LCX artery was also noted (not shown). The patient was assigned CAD-RADS 2, and no further imaging was recommended.

tests such as exercise electrocardiography, stress scintigraphy, stress echocardiography, stress MRI, or invasive fractional flow reserve are used for detection of stenosis (79). With advances in technology, evaluation of the hemodynamic significance of stenosis at CT is now possible with techniques such as CT perfusion, CT fractional flow reserve, and transluminal attenuation gradient imaging (80,81). In addition, regional wall motion abnormalities in a vascular distribution in a retrospective ECG-gated cine acquisition also indicate the presence of ischemia (Movies 1, 2). Myocardial ischemia and myocardial infarction can also be discovered incidentally at routine CT angiography or CT (Fig 34). However, CAD-RADS classification does not address these additional findings or other techniques that can provide hemodynamic significance.

Scenario 16: Incidental Noncoronary Findings

Case.—A 39-year-old man with chronic chest pain and intermediate risk for CAD underwent coronary CT angiography. No atherosclerotic plaques or stenosis was found, but an ovoid area of hypoattenuation was identified incidentally in the anterior mediastinum and was suspected to be a thymic lesion (Fig 35).

Comments.—Because of the absence of plaque or stenosis in all of the coronary arteries, the category assigned was CAD-RADS 0. A mediastinal lesion is not considered in determination of the CAD-RADS category or modifiers.

Incidental findings are abnormalities of potential clinical relevance that are unrelated to the main purpose of the evaluation (82). They are commonly detected at coronary CT angiography and involve different anatomic regions, depending on the field of view. One study (83) showed that an estimated 44% of patients had at least one noncardiac finding. The lung is the most common site of incidental findings, with lung nodules seen in 14% of patients who undergo coronary CT angiography (84). Incidental findings can also be seen in the mediastinum, breast, bones, and upper abdomen. Although most of these findings are benign and inconsequential, a small percentage of them are clinically significant, including potentially life-threatening conditions and malignancy. A pulmonary embolism can be seen in 0.2% (85) and aortic dissection in 1.1% of patients who undergo coronary CT angiography for acute chest pain (86). The prevalence of clinically significant findings is 10%–17% of patients (83,85,87), with an estimated malignancy rate of 0.3%–1.2% (83,87,88). The CAD-RADS guidelines do not specifically address incidental noncoronary findings. Given the wide variety of possible incidental findings, all the images should be evaluated for potentially clinically significant noncoronary findings. Further management may be determined according to preexisting guidelines for that specific finding. For example, lung nodules can be followed up on the basis of the 2017 Fleischner Society criteria for the management of incidental pulmonary nodules (89).

Current Status of CAD-RADS and Future Directions

To date, the adoption of CAD-RADS in clinical practice has been variable but promising (90). CAD-RADS has been shown to have high interobserver reproducibility, particularly with expert readers and high-quality images (91) (intraclass correlation coefficient, 0.958; 95%

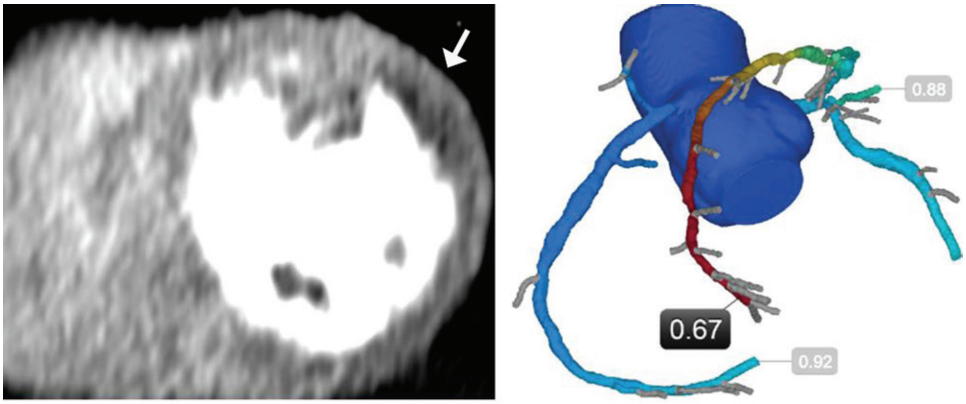

a. b.

Figure 33. Hemodynamic significance of stenosis in two patients. **(a)** Short-axis CT perfusion image after vasodilator stress with adenosine in a 53-year-old man with chest pain shows a perfusion defect in the anterolateral wall (arrow), which is consistent with myocardial ischemia. No defect was seen on CT perfusion images obtained with the patient at rest (not shown). **(b)** CT fractional flow reserve image in a 66-year-old man with stable angina and moderate stenosis in the LAD artery shows a CT fractional flow value of 0.67, which is abnormal. Currently, the CAD-RADS does not take into account the results of CT techniques for evaluation of myocardial ischemia.

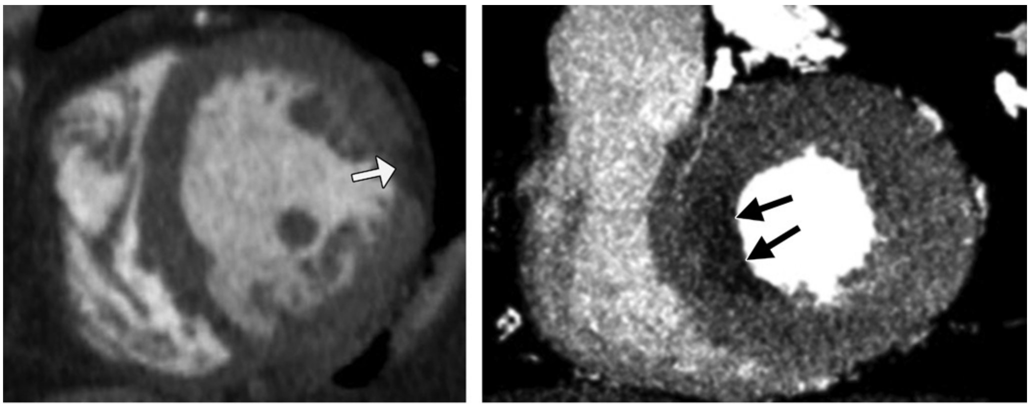

a. b.

Figure 34. Myocardial infarction in two patients. **(a)** Short-axis reconstruction of a cardiac CT image in a 63-year-old woman with CAD shows wall thinning and a focal hypoattenuating area in the lateral wall of the mid left ventricle (arrow), which is suggestive of remote myocardial infarction. **(b)** Short-axis reconstruction of a cardiac CT image in a 54-year-old man shows perfusion defects in the basal septum (arrows), which are consistent with previous myocardial infarction.

confidence interval, 0.938–0.974; $P < .0001$) (91), with one study showing good agreement for CAD-RADS 2 (92). Similarly, all modifiers had excellent agreement, except for V, which showed fair agreement (91,92). According to these results, there were no differences among the CAD-RADS categories for reader variability. Although a significant difference among readers was found in the evaluation of vulnerable plaque, the addition of modifier V does not change the recommended management. The CAD-RADS category is what matters, regardless of the presence of a modifier. Automated CAD-RADS classification with the use of data that readers enter manually is more accurate than manual classification, because human errors are lessened. Structured reporting systems with automated classification of CAD-RADS may improve data quality and enable standardization (93). One study (94) of 200 patients evaluated management of CAD after patients had undergone coronary CT angiography before the introduction of the CAD-RADS. For CAD-RADS categories at the ends of the spectrum (categories 0, 1, 2, 4, and 5), further testing was in accordance with CAD-RADS recommendations for 98% of patients. However, for CAD-RADS 3, 50% of patients were referred to undergo ICA and only 36% were referred for functional testing. Patients assigned the N category did not undergo further investigation. A study (95) of 5039 patients in the Coronary CT Angiography Evaluation for Clinical Outcomes (CONFIRM) study registry showed that incorporating CAD-RADS is an opportunity to provide evidence-based care after coronary CT angiography. In this study, the cumulative 5-year event-free survival rate correlated with the CAD-RADS category, ranging from 95.2% for category 0 and 0%–69.3% for category 5. The event risk was higher for higher categories (hazard ratio, 2.46–6.09). The receiver operating characteristic curve for the prediction of myocardial infarction or death was 0.7052, which is noninferior to results of the Duke index. ICA rates were also dependent on categories (13% for CAD-RADS 0 to 2, 66% for CAD-RADS 3, and 84% for CAD RADS ≥ 4A). Of the CAD-RADS 3 patients who received 30-day ICA, greater than 57% were asymptomatic or were not receiving antianginal therapy at baseline, whereas only 32% were undergoing antianginal or medical therapy (96).

Conclusion

CAD-RADS was modeled on other successful classification systems for the lung (Lung-RADS), breast (BI-RADS), and prostate (PI-RADS). The main goals of the CAD-RADS are to decrease variability between readers and enhance communication between interpreting and referring clinicians, with suggestions for the best course of action in patient care. There are several clinical situations that are not explicitly addressed by CAD-RADS and in which assignment of a CAD-RADS category is not straightforward. We have addressed these situations and have provided recommendations for their further patient care. Future iterations of CAD-RADS may address these scenarios.

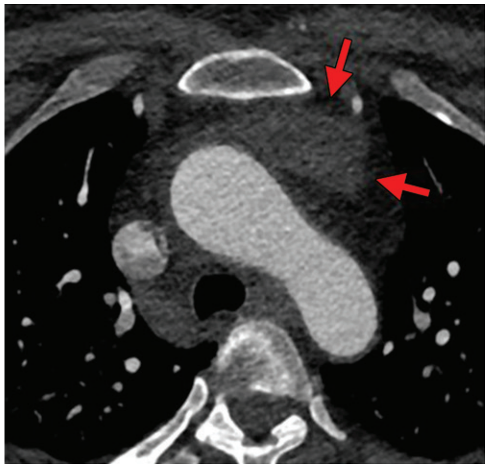

Figure 35. CAD-RADS 0 in a 39-year-old man with chronic chest pain. Coronary CT angiographic image shows no atherosclerotic CAD. An ovoid hypoattenuating mass (arrows) was seen incidentally in the anterior mediastinum, which is suggestive of a thymic lesion. Pathologic evaluation of the lesion revealed a benign multilocular thymic cyst with cholesterol cleft granulomas.

References

1. Cury RC. President's page: Ten years of innovation in cardiac CT. J Cardiovasc Comput Tomogr 2014;8(4):338–339.
2. Douglas PS, Hoffmann U, Patel MR, et al. Outcomes of anatomical versus functional testing for coronary artery disease. N Engl J Med 2015;372(14):1291–1300.
3. SCOT-HEART investigators. CT coronary angiography in patients with suspected angina due to coronary heart disease (SCOT-HEART): an open-label, parallel-group, multicentre trial. Lancet 2015;385(9985):2383–2391 [Published correction appears in Lancet 2015;385(9985):2354.] https://doi.org/10.1016/S0140-6736(15)60291-4.
4. Goldstein JA, Chinnaiyan KM, Abidov A, et al. The CT-STAT (Coronary Computed Tomographic Angiography for Systematic Triage of Acute Chest Pain Patients to Treatment) trial. J Am Coll Cardiol 2011;58(14):1414–1422.
5. Litt HI, Gatsonis C, Snyder B, et al. CT angiography for safe discharge of patients with possible acute coronary syndromes. N Engl J Med 2012;366(15):1393–1403.
6. Hoffmann U, Truong QA, Schoenfeld DA, et al. Coronary CT angiography versus standard evaluation in acute chest pain. N Engl J Med 2012;367(4):299–308.
7. Hamilton-Craig C, Fifoot A, Hansen M, et al. Diagnostic performance and cost of CT angiography versus stress ECG—a randomized prospective study of suspected acute coronary syndrome chest pain in the emergency department (CT-COMPARE). Int J Cardiol 2014;177(3):867–873.
8. Meijboom WB, van Mieghem CA, Mollet NR, et al. 64-slice computed tomography coronary angiography in patients with high, intermediate, or low pretest probability of significant coronary artery disease. J Am Coll Cardiol 2007;50(15):1469–1475.
9. Budoff MJ, Dowe D, Jollis JG, et al. Diagnostic performance of 64-multidetector row coronary computed tomographic angiography for evaluation of coronary artery stenosis in individuals without known coronary artery disease: results from the prospective multicenter ACCURACY (Assessment by Coronary Computed Tomographic Angiography of Individuals Undergoing Invasive Coronary Angiography) trial. J Am Coll Cardiol 2008;52(21):1724–1732.
10. Miller JM, Rochitte CE, Dewey M, et al. Diagnostic performance of coronary angiography by 64-row CT. N Engl J Med 2008;359(22):2324–2336.
11. National Institute for Health and Clinical Excellence. Chest pain of recent onset: assessment and diagnosis of recent onset chest pain or discomfort of suspected cardiac origin (update). CG95. London, England: National Institute for Health and Clinical Excellence, 2016.
12. Schmermund A, Eckert J, Schmidt M, Magedanz A, Voigtländer T. Coronary computed tomography angiography: a method coming of age. Clin Res Cardiol 2018;107(Suppl 2):40–48.
13. Nielsen LH, Ortner N, Nørgaard BL, Achenbach S, Leipsic J, Abdulla J. The diagnostic accuracy and outcomes after coronary computed tomography angiography vs. conventional functional testing in patients with stable angina pectoris: a systematic review and meta-analysis. Eur Heart J Cardiovasc Imaging 2014;15(9):961–971.
14. Rajiah P, Abbara S. CT coronary imaging-a fast evolving world. QJM 2018;111(9):595–604.
15. Cury RC, Abbara S, Achenbach S, et al. CAD-RADS(TM) Coronary Artery Disease - Reporting and Data System. An expert consensus document of the Society of Cardiovascular Computed Tomography (SCCT), the American College of Radiology (ACR) and the North American Society for Cardiovascular Imaging (NASCI). Endorsed by the American College of Cardiology. J Cardiovasc Comput Tomogr 2016;10(4):269–281.
16. Austen WG, Edwards JE, Frye RL, et al. A reporting system on patients evaluated for coronary artery disease. Report of the Ad Hoc Committee for Grading of Coronary Artery Disease, Council on Cardiovascular Surgery, American Heart Association. Circulation 1975;51(4 Suppl):5–40.
17. Raff GL, Abidov A, Achenbach S, et al. SCCT guidelines for the interpretation and reporting of coronary computed tomographic angiography. J Cardiovasc Comput Tomogr 2009;3(2):122–136.

18. Caussin C, Larchez C, Ghostine S, et al. Comparison of coronary minimal lumen area quantification by sixty-four-slice computed tomography versus intravascular ultrasound for intermediate stenosis. Am J Cardiol 2006;98(7):871–876.
19. Wijns W, Serruys PW, Reiber JH, et al. Quantitative angiography of the left anterior descending coronary artery: correlations with pressure gradient and results of exercise thallium scintigraphy. Circulation 1985;71(2):273–279.
20. Takagi A, Tsurumi Y, Ishii Y, Suzuki K, Kawana M, Kasanuki H. Clinical potential of intravascular ultrasound for physiological assessment of coronary stenosis: relationship between quantitative ultrasound tomography and pressure-derived fractional flow reserve. Circulation 1999;100(3):250–255.
21. Leipsic J, Abbara S, Achenbach S, et al. SCCT guidelines for the interpretation and reporting of coronary CT angiography: a report of the Society of Cardiovascular Computed Tomography Guidelines Committee. J Cardiovasc Comput Tomogr 2014;8(5):342–358.
22. Arbab-Zadeh A, Hoe J. Quantification of coronary arterial stenoses by multidetector CT angiography in comparison with conventional angiography methods, caveats, and implications. JACC Cardiovasc Imaging 2011;4(2):191–202.
23. Zhang S, Levin DC, Halpern EJ, Fischman D, Savage M, Walinsky P. Accuracy of MDCT in assessing the degree of stenosis caused by calcified coronary artery plaques. AJR Am J Roentgenol 2008;191(6):1676–1683.
24. Kalisz K, Buethe J, Saboo SS, Abbara S, Halliburton S, Rajiah P. Artifacts at Cardiac CT: Physics and Solutions. RadioGraphics 2016;36(7):2064–2083.
25. Sun Z, Ng CK, Xu L, Fan Z, Lei J. Coronary CT Angiography in Heavily Calcified Coronary Arteries: Improvement of Coronary Lumen Visualization and Coronary Stenosis Assessment With Image Postprocessing Methods. Medicine (Baltimore) 2015;94(48):e2148.
26. Morhard D, Fink C, Graser A, Reiser MF, Becker C, Johnson TR. Cervical and cranial computed tomographic angiography with automated bone removal: dual energy computed tomography versus standard computed tomography. Invest Radiol 2009;44(5):293–297.
27. Li P, Xu L, Yang L, et al. Blooming Artifact Reduction in Coronary Artery Calcification by A New De-blooming Algorithm: Initial Study. Sci Rep 2018;8(1):6945.
28. SCOT-HEART Investigators, Newby DE, Adamson PD, et al. Coronary CT Angiography and 5-Year Risk of Myocardial Infarction. N Engl J Med 2018;379(10):924–933.
29. Roger VL, Go AS, Lloyd-Jones DM, et al. Heart disease and stroke statistics--2012 update: a report from the American Heart Association. Circulation 2012;125(1):e2–e220 [Published correction appears in Circulation 2012;125(22):e1002.].
30. Alani A, Nakanishi R, Budoff MJ. Recent improvement in coronary computed tomography angiography diagnostic accuracy. Clin Cardiol 2014;37(7):428–433.
31. Zhao J, Zheng LL, Yang Y. Evaluation of coronary artery in-stent patency using 64-slice computed tomography. Coron Artery Dis 2011;22(8):540–552.
32. Malagutti P, Nieman K, Meijboom WB, et al. Use of 64-slice CT in symptomatic patients after coronary bypass surgery: evaluation of grafts and coronary arteries. Eur Heart J 2007;28(15):1879–1885.
33. Ropers D, Pohle FK, Kuettner A, et al. Diagnostic accuracy of noninvasive coronary angiography in patients after bypass surgery using 64-slice spiral computed tomography with 330-ms gantry rotation. Circulation 2006;114(22):2334–2341; quiz 2334.
34. Chan M, Ridley L, Dunn DJ, et al. A systematic review and meta-analysis of multidetector computed tomography in the assessment of coronary artery bypass grafts. Int J Cardiol 2016;221:898–905.
35. Puchner SB, Liu T, Mayrhofer T, et al. High-risk plaque detected on coronary CT angiography predicts acute coronary syndromes independent of significant stenosis in acute chest pain: results from the ROMICAT-II trial. J Am Coll Cardiol 2014;64(7):684–692.
36. Motoyama S, Sarai M, Harigaya H, et al. Computed tomographic angiography characteristics of atherosclerotic plaques subsequently resulting in acute coronary syndrome. J Am Coll Cardiol 2009;54(1):49–57.
37. Maurovich-Horvat P, Hoffmann U, Vorpahl M, Nakano M, Virmani R, Alkadhi H. The napkin-ring sign: CT signature of high-risk coronary plaques? JACC Cardiovasc Imaging 2010;3(4):440–444.
38. Obaid DR, Calvert PA, Brown A, et al. Coronary CT angiography features of ruptured and high-risk atherosclerotic plaques: Correlation with intra-vascular ultrasound. J Cardiovasc Comput Tomogr 2017;11(6):455–461.
39. Conley MJ, Ely RL, Kisslo J, Lee KL, McNeer JF, Rosati RA. The prognostic spectrum of left main stenosis. Circulation 1978;57(5):947–952.
40. Min JK, Shaw LJ, Devereux RB, et al. Prognostic value of multidetector coronary computed tomographic angiography for prediction of all-cause mortality. J Am Coll Cardiol 2007;50(12):1161–1170.
41. Williams M, Shaw LJ, Raggi P, et al. Prognostic value of number and site of calcified coronary lesions compared with the total score. JACC Cardiovasc Imaging 2008;1(1):61–69.
42. Cho SC, Park DW, Park SJ. Percutaneous Coronary Intervention and Coronary Artery Bypass Grafting for the Treatment of Left Main Coronary Artery Disease. Korean Circ J 2019;49(5):369–383.
43. Holmes DR Jr, Leon MB, Moses JW, et al. Analysis of 1-year clinical outcomes in the SIRIUS trial: a randomized trial of a sirolimus-eluting stent versus a standard stent in patients at high risk for coronary restenosis. Circulation 2004;109(5):634–640.
44. Sheth T, Dodd JD, Hoffmann U, et al. Coronary stent assessability by 64 slice multi-detector computed tomography. Catheter Cardiovasc Interv 2007;69(7):933–938.
45. Hecht HS, Gade C. Current and evolving stent evaluation by coronary computed tomographic angiography. Catheter Cardiovasc Interv 2011;77(6):843–859.
46. Kitagawa T, Yamamoto H, Horiguchi J, et al. Usefulness of measuring coronary lumen density with multi-slice computed tomography to detect in-stent restenosis. Int J Cardiol 2008;124(2):239–243.
47. Chung SH, Kim YJ, Hur J, et al. Evaluation of coronary artery in-stent restenosis by 64-section computed tomography: factors affecting assessment and accurate diagnosis. J Thorac Imaging 2010;25(1):57–63.
48. Boos J, Kröpil P, Lanzman RS, et al. Stent Lumen Visibility in Single-energy CT Angiography: Does Tube Potential Matter? Acad Radiol 2016;23(6):752–759.
49. Amanuma M, Kondo T, Sano T, et al. Assessment of coronary in-stent restenosis: value of subtraction coronary computed tomography angiography. Int J Cardiovasc Imaging 2016;32(4):661–670.
50. Marano R, Storto ML, Merlino B, Maddestra N, Di Giammarco G, Bonomo L. A pictorial review of coronary artery bypass grafts at multidetector row CT. Chest 2005;127(4):1371–1377.
51. Shiono Y, Kubo T, Honda K, et al. Impact of functional focal versus diffuse coronary artery disease on bypass graft patency. Int J Cardiol 2016;222:16–21.
52. de Graaf FR, van Velzen JE, Witkowska AJ, et al. Diagnostic performance of 320-slice multidetector computed tomography coronary angiography in patients after coronary artery bypass grafting. Eur Radiol 2011;21(11):2285–2296.
53. Heye T, Kauczor HU, Szabo G, Hosch W. Computed tomography angiography of coronary artery bypass grafts: robustness in emergency and clinical routine settings. Acta Radiol 2014;55(2):161–170.
54. Laspas F, Roussakis A, Kritikos N, Mourmouris C, Efthimiadou R, Andreou J. Imaging of coronary artery bypass grafts by computed tomography coronary angiography. Curr Probl Diagn Radiol 2013;42(6):241–248.
55. Feuchtner G, Kerber J, Burghard P, et al. The high-risk criteria low-attenuation plaque <60 HU and the napkin-ring sign are the most powerful predictors of MACE: a long-term follow-up study. Eur Heart J Cardiovasc Imaging 2017;18(7):772–779.
56. Motoyama S, Ito H, Sarai M, et al. Plaque Characterization by Coronary Computed Tomography Angiography and the

Likelihood of Acute Coronary Events in Mid-Term Follow-Up. J Am Coll Cardiol 2015;66(4):337–346.
57. Otsuka K, Fukuda S, Tanaka A, et al. Napkin-ring sign on coronary CT angiography for the prediction of acute coronary syndrome. JACC Cardiovasc Imaging 2013;6(4):448–457.
58. Hecht HS, Polena S, Jelnin V, et al. Stent gap by 64-detector computed tomographic angiography relationship to in-stent restenosis, fracture, and overlap failure. J Am Coll Cardiol 2009;54(21):1949–1959.
59. Williams PD. Stent fracture with contemporary coronary stent platforms. EuroIntervention 2014;10(5):651–652.
60. Lee MS, Jurewitz D, Aragon J, Forrester J, Makkar RR, Kar S. Stent fracture associated with drug-eluting stents: clinical characteristics and implications. Catheter Cardiovasc Interv 2007;69(3):387–394.
61. Aoki J, Nakazawa G, Tanabe K, et al. Incidence and clinical impact of coronary stent fracture after sirolimus-eluting stent implantation. Catheter Cardiovasc Interv 2007;69(3):380–386.
62. Pflederer T, Marwan M, Schepis T, et al. Characterization of culprit lesions in acute coronary syndromes using coronary dual-source CT angiography. Atherosclerosis 2010;211(2):437–444.
63. Dey D, Achenbach S, Schuhbaeck A, et al. Comparison of quantitative atherosclerotic plaque burden from coronary CT angiography in patients with first acute coronary syndrome and stable coronary artery disease. J Cardiovasc Comput Tomogr 2014;8(5):368–374.
64. Bauer RW, Thilo C, Chiaramida SA, Vogl TJ, Costello P, Schoepf UJ. Noncalcified atherosclerotic plaque burden at coronary CT angiography: a better predictor of ischemia at stress myocardial perfusion imaging than calcium score and stenosis severity. AJR Am J Roentgenol 2009;193(2):410–418.
65. Baltaxe HA, Wixson D. The incidence of congenital anomalies of the coronary arteries in the adult population. Radiology 1977;122(1):47–52.
66. Yamanaka O, Hobbs RE. Coronary artery anomalies in 126,595 patients undergoing coronary arteriography. Cathet Cardiovasc Diagn 1990;21(1):28–40.
67. Cheezum MK, Ghoshhajra B, Bittencourt MS, et al. Anomalous origin of the coronary artery arising from the opposite sinus: prevalence and outcomes in patients undergoing coronary CTA. Eur Heart J Cardiovasc Imaging 2017;18(2):224–235.
68. Warnes CA, Williams RG, Bashore TM, et al. ACC/AHA 2008 guidelines for the management of adults with congenital heart disease: a report of the American College of Cardiology/American Heart Association Task Force on Practice Guidelines (Writing Committee to Develop Guidelines on the Management of Adults With Congenital Heart Disease). Developed in Collaboration With the American Society of Echocardiography, Heart Rhythm Society, International Society for Adult Congenital Heart Disease, Society for Cardiovascular Angiography and Interventions, and Society of Thoracic Surgeons. J Am Coll Cardiol 2008;52(23):e143–e263.
69. Dodd JD, Ferencik M, Liberthson RR, et al. Congenital anomalies of coronary artery origin in adults: 64-MDCT appearance. AJR Am J Roentgenol 2007;188(2):W138–W146.
70. Cheezum MK, Liberthson RR, Shah NR, et al. Anomalous Aortic Origin of a Coronary Artery From the Inappropriate Sinus of Valsalva. J Am Coll Cardiol 2017;69(12):1592–1608.
71. Waller BF, Fry ET, Hermiller JB, Peters T, Slack JD. Nonatherosclerotic causes of coronary artery narrowing: Part I. Clin Cardiol 1996;19(6):509–512.
72. Waller BF, Fry ET, Hermiller JB, Peters T, Slack JD. Nonatherosclerotic causes of coronary artery narrowing: Part II. Clin Cardiol 1996;19(7):587–591.
73. Fabris E, Kilic ID, Caiazzo G, et al. Nonatherosclerotic Coronary Artery Narrowing. JACC Cardiovasc Imaging 2016;9(3):317–320.
74. Waller BF, Fry ET, Hermiller JB, Peters T, Slack JD. Nonatherosclerotic causes of coronary artery narrowing: Part III. Clin Cardiol 1996;19(8):656–661.
75. Díaz-Zamudio M, Bacilio-Pérez U, Herrera-Zarza MC, et al. Coronary artery aneurysms and ectasia: role of coronary CT angiography. RadioGraphics 2009;29(7):1939–1954.
76. Pahlavan PS, Niroomand F. Coronary artery aneurysm: a review. Clin Cardiol 2006;29(10):439–443.
77. Swaye PS, Fisher LD, Litwin P, et al. Aneurysmal coronary artery disease. Circulation 1983;67(1):134–138.
78. Chandrashekhar Y, Min JK, Hecht H, Narula J. CAD-RADS: A Giant First Step Toward a Common Lexicon? JACC Cardiovasc Imaging 2016;9(9):1125–1129.
79. Mangiacapra F, Bressi E, Sticchi A, Morisco C, Barbato E. Fractional flow reserve (FFR) as a guide to treat coronary artery disease. Expert Rev Cardiovasc Ther 2018;16(7):465–477.
80. Hamon M, Geindreau D, Guittet L, Bauters C, Hamon M. Additional diagnostic value of new CT imaging techniques for the functional assessment of coronary artery disease: a meta-analysis. Eur Radiol 2019;29(6):3044–3061.
81. Cademartiri F, Seitun S, Clemente A, et al. Myocardial blood flow quantification for evaluation of coronary artery disease by computed tomography. Cardiovasc Diagn Ther 2017;7(2):129–150.
82. O'Sullivan JW, Muntinga T, Grigg S, Ioannidis JPA. Prevalence and outcomes of incidental imaging findings: umbrella review. BMJ 2018;361:k2387.
83. Flor N, Di Leo G, Squarza SA, et al. Malignant incidental extracardiac findings on cardiac CT: systematic review and meta-analysis. AJR Am J Roentgenol 2013;201(3):555–564.
84. Robertson J, Nicholls S, Bardin P, Ptasznik R, Steinfort D, Miller A. Incidental Pulmonary Nodules Are Common on CT Coronary Angiogram and Have a Significant Cost Impact. Heart Lung Circ 2019;28(2):295–301.
85. Williams MC, Hunter A, Shah ASV, et al. Impact of noncardiac findings in patients undergoing CT coronary angiography: a substudy of the Scottish computed tomography of the heart (SCOT-HEART) trial. Eur Radiol 2018;28(6):2639–2646.
86. Burris AC 2nd, Boura JA, Raff GL, Chinnaiyan KM. Triple Rule Out Versus Coronary CT Angiography in Patients With Acute Chest Pain: Results From the ACIC Consortium. JACC Cardiovasc Imaging 2015;8(7):817–825.
87. Karius P, Schuetz GM, Schlattmann P, Dewey M. Extracardiac findings on coronary CT angiography: a systematic review. J Cardiovasc Comput Tomogr 2014;8(3):174–182.e1–e6.
88. Earls JP. The pros and cons of searching for extracardiac findings at cardiac CT: studies should be reconstructed in the maximum field of view and adequately reviewed to detect pathologic findings. Radiology 2011;261(2):342–346.
89. MacMahon H, Naidich DP, Goo JM, et al. Guidelines for Management of Incidental Pulmonary Nodules Detected on CT Images: From the Fleischner Society 2017. Radiology 2017;284(1):228–243.
90. Dewey M. Structure or entropy in reporting cardiac CT findings. Int J Cardiovasc Imaging 2016;32(11):1657–1658.
91. Maroules CD, Hamilton-Craig C, Branch K, et al. Coronary artery disease reporting and data system (CAD-RADSTM): Inter-observer agreement for assessment categories and modifiers. J Cardiovasc Comput Tomogr 2018;12(2):125–130.
92. Abdel Razek AAK, Elrakhawy MM, Yossof MM, Nageb HM. Inter-observer agreement of the Coronary Artery Disease Reporting and Data System (CAD-RADSTM) in patients with stable chest pain. Pol J Radiol 2018;83:e151–e159.
93. Szilveszter B, Kolossváry M, Karády J, et al. Structured reporting platform improves CAD-RADS assessment. J Cardiovasc Comput Tomogr 2017;11(6):449–454.
94. Guerreiro S, Ferreira AM, Abecasis J, et al. Additional cardiac investigation prior to the introduction of the CAD-RADS classification in coronary computed tomography angiography reports. Rev Port Cardiol 2019;38(1):45–50.
95. Xie JX, Cury RC, Leipsic J, et al. The Coronary Artery Disease-Reporting and Data System (CAD-RADS): Prognostic and Clinical Implications Associated With Standardized Coronary Computed Tomography Angiography Reporting. JACC Cardiovasc Imaging 2018;11(1):78–89.